

Production of Biodiesel from Algae

A Technical Report submitted to the Department of Chemical Engineering

Presented to the Faculty of the School of Engineering and Applied Science

University of Virginia • Charlottesville, Virginia

In Partial Fulfillment of the Requirements for the Degree
Bachelor of Science, School of Engineering and Applied Science

Spring, 2022

Technical Project Team Members

Avery Black

Joey Kwon

Thomas “Hunter” O’Quinn

Kazu Yoshizaki

On my honor as a University Student, I have neither given nor received unauthorized aid on this
assignment as defined by the Honor Guidelines for Thesis-Related Assignments

Eric Anderson, Department of Chemical Engineering

Table of Contents

Executive Summary	7
1. Introduction	9
1.1 Background	9
1.2. Product Description	10
1.3 Starting Materials	11
1.4 Scale	12
1.4.1 Biodiesel Production	12
1.4.2 Glycerol Production	12
2. Discussion	13
2.1 Algae Strain	14
2.2 Nutrient Source for Algae Cultivation	14
2.3 Nutrient Extraction	14
2.4 Growth Conditions for <i>C. Vulgaris</i>	15
2.5 Photobioreactor Design Considerations	19
2.6 Raceway Pond Design Considerations	20
2.7 Dissolved Air Flotation	21
2.8 Cell Disruption	22
2.8.1 Acid Disruption	22
2.8.2 High Pressure Homogenization	23
2.9 Biomass Drying	23
2.9.1 Sludge-Dewatering Step	23
2.9.2 Conveyor Belt Drying	24
2.10 Lipid Extraction using Hexane	25
2.11 Hexane Recovery	26
2.12 Acid Esterification	28
2.12.1 Esterification Material Balances	28
2.13 Post Esterification Methanol Recovery	30
2.13.1 Design Specifications and Process Design	30
2.14 Base Transesterification	32
2.14.1 Trans-Esterification Material Balances	32
2.14.2 Trans-Esterification Reactor Design Considerations	33
2.15 Glycerol/Biodiesel Separation	34
2.16 Post Trans-esterification Methanol Recovery	34
2.17 Biodiesel Washing	35

2.17.1 Biodiesel Specifications and Process Design	35
2.18 Biodiesel Drying	36
2.19 Neutralization	36
2.20 Glycerol Purification	37
2.20.1 Glycerol Vacuum Distillation	38
3. Recommended Design	39
3.1 Nutrient Extraction	40
3.1.1 Mixer Design (M-101)	40
3.1.2 Settler Design (S-101)	40
3.2 Raceway Design (R-201)	42
3.3 Dissolved Air Flotation (S-301) & Sludge Dewatering	43
3.4 Lipid Extraction	46
3.4.1 High Pressure Homogenization (M-401)	47
3.4.2 Biomass Drying (E-402)	47
3.4.3 Hexane Extraction (S-401)	49
3.4.4 Hexane Recovery (S-402)	49
3.5 Acid Pre-Esterification	51
3.5.1 Acid Reactor (R-501)	53
3.5.2 Settler (S-501)	54
3.5.3 Post-Acid Methanol Recovery Column (T-501)	55
3.5.4 Acid Flash Column (F-501)	57
3.6 Base Trans-Esterification	58
3.6.1 Base Reactor (R-601)	59
3.6.2 Methanol Flash Column (F-601)	60
3.6.3 Settler (S-602)	62
3.7 Biodiesel Purification	63
3.7.1 Wet Washing (S-701)	64
3.7.3 Biodiesel Drying (F-701)	65
3.8 Glycerol Purification	66
3.8.1 Glycerol Neutralization	67
3.8.2 Glycerol Flash Separation (F-801)	67
3.8.3 Glycerol Vacuum Distillation (T-801)	69
3.9 Ancillary Equipment	71
3.9.1 Pumps and Compressors	71
3.9.2 Heat Exchangers	74
3.9.3 Storage Tanks	75
3.10 Batch Operation Schedule	76

4. Economic Considerations	77
4.1 Total Capital Costs	77
4.1.1 Land	77
4.1.2 Nutrient Extraction	78
4.1.3 Algae Cultivation	78
4.1.4 Dissolved Air Flotation	80
4.1.5 Lipid Extraction	81
4.1.6 Acid Esterification Equipments	82
4.1.7 Transesterification Equipments	84
4.1.8 Refinement Equipment	85
4.1.9 Ancillary Equipment	87
4.1.10 Working Capital	91
4.1.11 Total Capital Costs	92
4.2 Yearly Operating Costs	93
4.2.1 Raw Material Costs	93
4.2.2 Utility Costs: Electricity	94
4.2.3 Utility Costs: Steam/Chilled Water	96
4.2.4 Labor Costs	98
4.2.5 Operating Costs and Product Revenue	100
4.2.6 Taxes and Other Fees	101
4.3 Cash Flow Analysis	102
4.4 Scenarios	104
4.4.1 Increased Diesel Price	104
4.4.2 Free Poultry Litter	106
4.4.3 Eliminate Glycerol Refinement	108
5. Safety and Environmental Concerns	111
5.1 Health and Safety Considerations	111
5.2 Environmental Considerations	113
5.3 Societal Considerations	116
6. Conclusions and Recommendations	118
7. Acknowledgements	119
References	120

List of Figures

Figure 1-2-01: Chemical Structure of FAME	10
Figure 1-2-02: Chemical Structure of Glycerol	11
Figure 2-0-01: Block Flow Diagram of Biodiesel Production	13
Figure 2-4-01: Monthly High, Low, and Average Temperature for Rockingham County, VA.	16
Figure 2-4-02: Average Light Intensity in Harrisonburg, Virginia	17
Figure 2-4-03: Growth Profiles of Chlorella. sp L1	18
Figure 2-7-01: Industrial Scale DAF Unit	22
Figure 2-10-01: Structure of Triolein	25
Figure 2-10-02: Structure of Oleic Acid	25
Figure 2-12-01: Acid Catalyzed Esterification Reaction	28
Figure 2-13-01: Block Flow Diagram for Methanol and Acid Recovery	30
Figure 2-14-01: Transesterification with Base Catalyst	32
Figure 2-14-02: Sequential Experimentation to Optimize Reactor Conditions	33
Figure 2-17-01: Amount of NaOH in Feed Stream After Washing	36
Figure 2-19-01: Neutralization Reaction	37
Figure 3-1-01: Nutrient Extraction, Raceway Pond, DAF Process Flow Diagram	39
Figure 3-2-01: Raceway Pond Layout	42
Figure 3-2-02: Configuration of Raceway Ponds	42
Figure 3-4-01: Lipid Extraction Process Flow Diagram	46
Figure 3-5-01: Acid Pre-Esterification Flow Diagram	51
Figure 3-5-02: Scale Up Equations for CSTRs	53
Figure 3-6-01: Base Trans-esterification Flow Diagram	58
Figure 3-7-01: Biodiesel Purification Flow Diagram	63
Figure 3-8-01: Glycerol Purification Flow Diagram	66
Figure 4-3-01: Cumulative Discounted Cash Flow Diagram	103
Figure 4-4-01: Cumulative Discounted Cash Flow Diagram (Higher Biodiesel Price)	105
Figure 4-4-02: Cumulative Discounted Cash Flow Diagram (Free Poultry Litter)	107
Figure 4-4-03: Cumulative Discounted Cash Flow Diagram (No Glycerol Refinement)	109

List of Tables

Table 3-1-01: Physical Dimensions of Nutrient Mixer	40
Table 3-1-02: Nutrient Extraction Stream Table	41
Table 3-2-01: Raceway Pond Stream Table	43
Table 3-3-01: DAF Separation & Sludge Dewatering Stream Table	44
Table 3-4-01: Heat Exchanger Specifications for E-401	48
Table 3-4-02: Homogenization & Drying Stream Table	48
Table 3-4-03: Hexane Extraction Decanter Stream Table	49
Table 3-4-04: Hexane Flash Separation Stream Table	50
Table 3-5-01: Acid Reactor Stream Table	52
Table 3-5-02: Acid Settler Stream Table	54
Table 3-5-03: Acid/Methanol Recovery Distillation Stream Table	55
Table 3-5-04: Acid Flash Separation Stream Table	57
Table 3-6-01: Trans-esterification Reactor Stream Table	60
Table 3-6-02: Trans-esterification Methanol Recovery Stream Table	61
Table 3-6-03: Glycerol/FAME Separation Stream Table	62
Table 3-7-01: Wet Washing Stream Table	64
Table 3-7-02: Biodiesel Drying Stream Table	65
Table 3-8-01: Glycerol-Acid Neutralization Stream Table	67
Table 3-8-02: Glycerol Flash Separation Stream Table	68
Table 3-8-03: Glycerol Vacuum Distillation Stream Table	70
Table 3-9-01: Pump Specifications	71,72
Table 3-9-02: Example Specifications Needed for Pump Design	73
Table 3-9-03: Compressor Specifications	73
Table 3-9-04: Heat Exchanger Specifications	74
Table 3-9-05: Storage Tanks	75
Table 4-1-01: Land Cost	77
Table 4-1-02: Nutrient Extraction Equipment	78
Table 4-1-03: Cost of Creating Ponds	78
Table 4-1-04: Cost of PVC Liner	79
Table 4-1-05: Cost of Paddlewheel	79
Table 4-1-06: Total Cost of Raceway Pond Installation	79
Table 4-1-07: DAF Unit Model Specifications	80
Table 4-1-08: Cost of DAF Equipment	80
Table 4-1-09: Estimated Price of GEA Ariete Homogenizer	81
Table 4-1-10: Scaled Price of Biomass Dryer	81
Table 4-1-11: Hexane Extraction and Hexane Recovery	82
Table 4-1-12: Cost of Acid Esterification Reactor	82
Table 4-1-13: Cost of Post-Esterification Separation Equipment	83

Table 4-1-14: Cost of Base Trans-esterification Reactor	84
Table 4-1-15: Cost of Post-Trans-esterification Separation Equipment	84
Table 4-1-16: Cost of Biodiesel Refinement Equipment	85
Table 4-1-17: Cost of Glycerol Refinement Equipment	86
Table 4-1-18: Cost of Pumps and Compressors	87,88
Table 4-1-19: Cost of Heat Exchangers	89
Table 4-1-20: Cost of Storage Tanks	90
Table 4-1-21: Working Capital Costs	91
Table 4-1-22: Capital Costs Breakdown	92
Table 4-2-01: Raw Material Costs	93
Table 4-2-02: Pumps and Compressors Operating Costs	94,95
Table 4-2-03: Condenser Operating Costs	96
Table 4-2-04: Heater Operating Costs	97
Table 4-2-05: Number of Process Steps	98
Table 4-2-06: Labor Costs for Operators and Supervisors	99
Table 4-2-07: Total Yearly Operating Costs	100
Table 4-2-08: Total Yearly Product Revenue	100
Table 4-3-01: Operating Cash Flow	102
Table 4-4-01: Total Yearly Product Revenue (Higher Biodiesel Price)	104
Table 4-4-02: Operating Cash Flow (Higher Biodiesel Price)	104
Table 4-4-03: Yearly Operating Costs (Free Poultry Litter)	106
Table 4-4-04: Operating Cash Flow (Free Poultry Litter)	106
Table 4-4-05: Capital Saved from Eliminating Glycerol Refinement Process	108
Table 4-4-06: Labor Requirement (No Glycerol Refinement)	108
Table 4-4-07: Total Operating Costs (No Glycerol Refinement)	109
Table 4-4-08: Total Yearly Product Revenue (No Glycerol Refinement)	109

Executive Summary

This paper describes the design of an algae farm and biodiesel refinery. Kinetic data, Aspen Plus modeling, and other key chemical engineering considerations were used to create this design. The motivation for attempting to design this plant is two-fold. Firstly, it provides a means of obtaining a green fuel source that competes with fossil fuels through the production of biodiesel. Secondly, it uses poultry litter as a nutrient source, which will help prevent the nutrients from entering natural waterways and causing damage. An economic analysis was performed on the design in order to determine the feasibility of its implementation. This analysis involved the equipment cost, labor and benefits costs, utility costs, raw material costs, and taxes.

The process described in this paper begins with the extraction of nutrients from poultry litter, which are then used to grow *Chlorella Vulgaris* in open raceway ponds. Dissolved air flotation is then used to separate the algae from a portion of the water that it was grown in. The biomass is then disrupted by high pressure homogenization (HPH) in order to allow for a more effective lipid extraction. The lipids are then extracted using hexane, and the excess hexane is recycled back to the lipid extraction stage. The lipids then go through a pre-esterification reaction and trans-esterification reaction in order to convert them into fatty acid methyl esters (FAME). After both of these reactions, methanol recovery occurs to recycle the unreacted methanol back into each of the reactors. The biodiesel, also known as FAME, is then refined through the use of wet washing and drying using a flash drum. The crude glycerol produced as a by-product is neutralized, and then it is refined using a flash drum and vacuum distillation.

The plant is assumed to operate on a yearly schedule where production scale is proportional to the algae growth rate. In a year of production, 4.5 MM gallons of biodiesel and 970,000 kg of

glycerol will be produced, which at a rate of \$2.50/gallon biodiesel and \$0.73/kg glycerol, brings in a yearly product revenue of \$12 MM. As designed, the plant costs \$297 MM in capital, \$22 MM in yearly operating cost, and \$6.2 MM in labor cost. Operating the plant during production years results in a loss of \$15.9 MM per year. Assuming a plant life of 20 years, the internal rate of return on this project will be -10.3%.

Given the rate of return on this project, the current design does not make it an economically viable project. However, three alternate scenarios are discussed in this report (increased diesel prices, free poultry litter, and elimination of glycerol refinement processes) which may help to make this process more economically attractive. The only scenario where this project may be economically feasible is when diesel prices are sold at \$14.25/gallon, at which point the investment breaks even at the end of the plant life.

1. Introduction

1.1 Background

Climate change has recently become a predominant problem; biofuels are a potential solution due to their absorption of carbon dioxide from the atmosphere. Biodiesel produced from algae will be the focus of this project; this project will address the need for an environmentally friendly fuel source that is able to meet the necessary specifications. Biodiesel has the potential to be used within existing infrastructure, which is partially due to its ability to be used in existing diesel motors. In the 1890's, the diesel engine was developed as the engine of choice for power, reliability, and its high fuel economy. Modern biodiesel fuel is made by converting vegetable oils into fatty acid methyl esters, research that was rooted in 1930's Belgium. As a competitor to the widespread availability and cost of petroleum diesel, biodiesel had low demand except in times of high oil prices and shortages. Due to its clean emissions profile and ease of adoption, the future of biofuels relies mostly on the world's ability to grow renewable feedstock. Algae biodiesel has a strong value proposition for cultivation efficiency because it performs photosynthesis 20-30 times faster than conventional crops.

The preliminary design for the algae cultivation process involved the simultaneous use of a closed photobioreactor and open raceway pond, unlike the traditional large-scale method of just an open raceway pond. Research supports that hybrid systems outperform isolated systems in algae growth and productivity (Narala, 2016). However, upon further research into the design and economics of the cultivation process, the design was shifted away from the hybrid cultivation method and towards just an open raceway pond, as the former was more complex and expensive than the latter. The goal of this project is to design a system which delivers biodiesel at a

comparable wholesale price to that of petroleum diesel, which is around \$2.50/gallon (U.S. Energy, n.d.). If comparable wholesale prices are achieved, algae biofuels would become a favorable alternative fuel.

1.2. Product Description

Biodiesel in the form of fatty acid methyl esters (FAME) is the desired product of the proposed process. The chemical formula of FAME is $\text{CH}_3(\text{CH}_2)_n\text{COOCH}_3$ and is characterized by having a hydrocarbon chain with a methyl ester group on one end (EBTP, 2011).

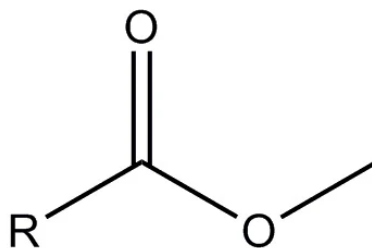


Figure 1-2-01: Chemical Structure of FAME

As an alternative source of renewable fuel, biodiesel is mainly used as transportation fuel. It has similar physical properties to that of conventional diesel, but it is biodegradable and non-toxic (EBTP, 2011). The biodiesel produced from this process will have to adhere to the standards set forth by the ASTM D6751 (U.S. Energy, n.d.). The cloud point of biodiesel has prevented its use in colder climates and occurs at a higher temperature than the cloud point of petrochemical based fuels.

As part of the transesterification reaction, a co-product of the proposed process is glycerol. The chemical formula for glycerol is $\text{C}_3\text{H}_8\text{O}_3$ (NCBI, 2021). The purified glycerol produced can be used for applications in various industries, such as the food, cosmetic, and the oleochemical industries. Glycerol can be used as a substrate for anaerobic digestion as well (EBTP, 2011).. The

desired purity of any glycerol produced as a byproduct is 99.5% or above. This will qualify it as USP grade, which allows it to have the greatest flexibility and use due to it meeting lower-grade requirements (US International Trade Commission, 2017).

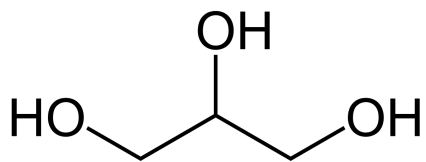


Figure 1-2-02: Chemical Structure of Glycerol

1.3 Starting Materials

The algae strain chosen for this process is *Chlorella vulgaris*, due to its high growth rate and high lipid content in nitrogen stressed conditions (Rodolfi, 2008). In addition, based on the volume of literature available for use, the growth behavior of *Chlorella vulgaris* was deemed to be well documented under various conditions.

The algae will be grown in an open raceway pond. The source of nutrients necessary for the growth of algae, both nitrogen and phosphorus, will come from chicken litter acquired from the Shenandoah Valley region. Water will be necessary for multiple parts of the process, such as nutrient extraction from the chicken litter and for growing the algae; currently, the plan is to recycle most of the water from algae cultivation to conserve materials. Sunlight will be used as the light source needed for algae growth in the raceway pond.

In the raceway ponds, the algae will be grown under nutrient-deficient conditions to promote lipogenesis (Adesanya, 2014). Because of this, water containing dilute nutrient concentrations will be required for the raceway pond. Air will be used for the carbon source to supplement the algae's growth and allow for photosynthesis. Air will be needed for dissolved air flotation (DAF), and no flocculant is needed as long as an approximate concentration of 500 mg/L

of algae is achieved (Niaghi, 2015). Hot air will be needed to dry the algae after it is removed from the water. Hexane will be used as an organic solvent to extract lipids from the dried algae; hexane was chosen due to it currently being the most economical option for lipid extraction (Patel, 2021). The first catalyst that will be used in the transesterification reaction will be sulfuric acid (H_2SO_4). Potassium hydroxide (KOH) will be used as the second catalyst for the transesterification reaction due to it being commonly used and having an ample amount of data being available for it. Methanol will be used as a reactant for the transesterification reaction. Methanol tends to be preferred over other alcohols due to its chemical and physical advantages (Musa, 2016). HCl will also be required for the acid washing of the biodiesel in an attempt to purify it.

1.4 Scale

1.4.1 Biodiesel Production

Based on this process' design, the yearly production of biodiesel at this plant will be around 14,070,000 kg. Assuming the biofuel has a relative density of 821 kg/m^3 (Nwanya, 2021), there would be a yearly production of m^3 . Based on this estimation, it is projected that the plant will produce approximately 4,528,000 gallons of biodiesel per year.

1.4.2 Glycerol Production

Based on this process' design, the yearly production of glycerol at this plant will be around 969,400 kg. Assuming the density of glycerol is around $1,260 \text{ kg/m}^3$, there would be a yearly production of 769.3 m^3 , which means there is approximately 203,200 gallons of high-grade glycerol produced per year.

2. Discussion

The overall block flow diagram of the algae biofuel production process is outlined below. It is broken up into four components, the upstream cultivation, lipid extraction, esterification and transesterification reactions, and refinement processes.

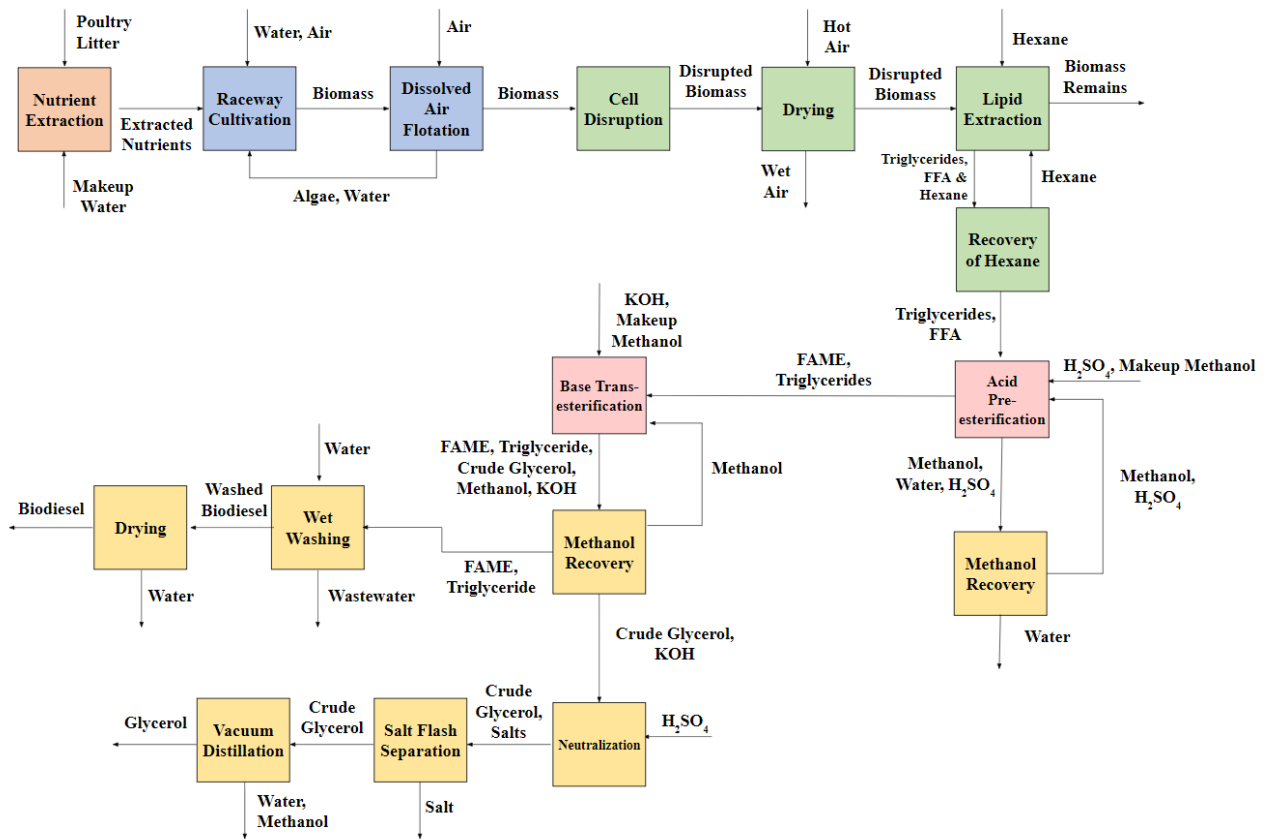


Figure 2-0-01: Block Flow Diagram of Biodiesel Production

2.1 Algae Strain

The strain of algae chosen for the production of biodiesel was *Chlorella Vulgaris*. *Chlorella Vulgaris* has a high growth rate and high lipid content in nitrogen stressed conditions (Rodolfi, 2008). In addition, based on the volume of literature available for use, the growth behavior of *Chlorella vulgaris* was deemed to be well documented under various conditions.

2.2 Nutrient Source for Algae Cultivation

The source of nutrients necessary for the growth of algae, both nitrogen and phosphorus, will come from poultry litter acquired from Augusta, Rockingham, Shenandoah, and Page county in the Shenandoah Valley region of Virginia. This source and location was selected as the Virginia Department of Conservation and Recreation offers the Virginia Poultry Litter Transport Incentive Program, where, depending on the plant location, transportation costs are offset by a certain amount to promote the development of self-sustaining poultry litter markets. Approximately 196,700 tons of chicken litter and 148,800 tons of turkey litter can be recovered per year across four counties that lie in the Shenandoah Valley region. (Fears, 2017). Assuming a concentration of 72 pounds of nitrogen per ton of chicken litter and 54 pounds of nitrogen per ton of turkey litter, this would mean there is access to approximately 30.4 tons of nitrogen per day (Chastain, 2003). *Chlorella vulgaris* is assumed to be made of 5.6% of elemental nitrogen (Vassilev, 2016). Based on this, it is expected that there is enough nitrogen available to support the growth of approximately 542 tons of algae per day.

2.3 Nutrient Extraction

Chicken and turkey litter sourced from the Shenandoah Valley will be used to create a nutrient broth used to supplement the growth of algae in the raceway ponds. To extract nutrients

and form a nutrient broth, the litter will first be mixed with water and agitated, then the mixture will be allowed to settle and the supernatant collected, which will be sent to the raceway ponds. The mixer will be designed according to standard configurations for CSTR's.

2.4 Growth Conditions for *C. Vulgaris*

The set-up explained by He et al. will be used to model the growth of *C. vulgaris* in the raceway ponds. Although He et al. shares some operating conditions used to cultivate the algae in the raceway ponds, no relevant information on temperature, light intensity, or pH is available. Therefore, optimal conditions of these parameters for the growth of *C. vulgaris* will be investigated.

To ensure the abundant growth of algae in the raceway ponds, optimal growth conditions for *Chlorella vulgaris* will be maintained according to reported conditions in Ru et al. The plant will be located in Rockingham County, VA.

At lower temperatures (below 16 °C), algae growth is limited. At higher temperatures, the metabolic rate of the algae increases, up to 35 °C, where algae growth is inhibited (Ru et al., 2020). The optimal temperature for cultivation of *C. vulgaris* is reported to be 20–30 °C, where 30 °C yields optimum biomass production and 25 °C yields optimum lipid production (Ru et al., 2020). Figure 2-4-01 shows the high, low, and average temperatures of Rockingham County, VA over the year. There is a four month window (June–September) where the average temperature falls within the optimum range. In the months where the average temperature falls outside the optimum range for algae growth, the cultivation will be assumed to yield a fraction of the peak productivity.

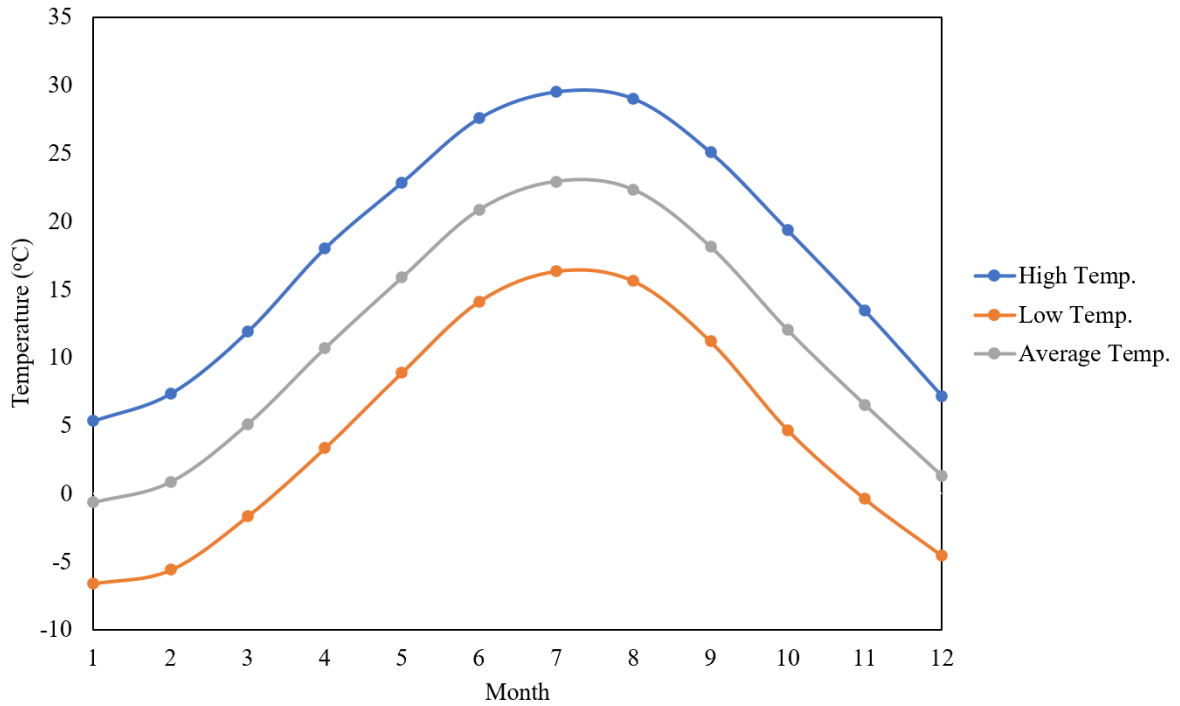


Figure 2-4-01: Monthly High, Low, and Average Temperature for Rockingham County, VA.

(Climate in Rockingham County, Virginia, n.d.)

For light intensity, the optimal conditions reported were 100–200 $\mu\text{mol photons/m}^2/\text{s}$, or 35–70 W/m^2 (Ru et al., 2020). Figure 2-4-02 shows the average light intensities in Harrisonburg, VA. Given that Harrisonburg is located near Rockingham County, the data reported in Figure 2-4-02 will be used to estimate the light intensities at the plant location. The light intensities, which range from 92–288 W/m^2 throughout the year, are consistently above the optimum range for algae growth reported by Ru et al.

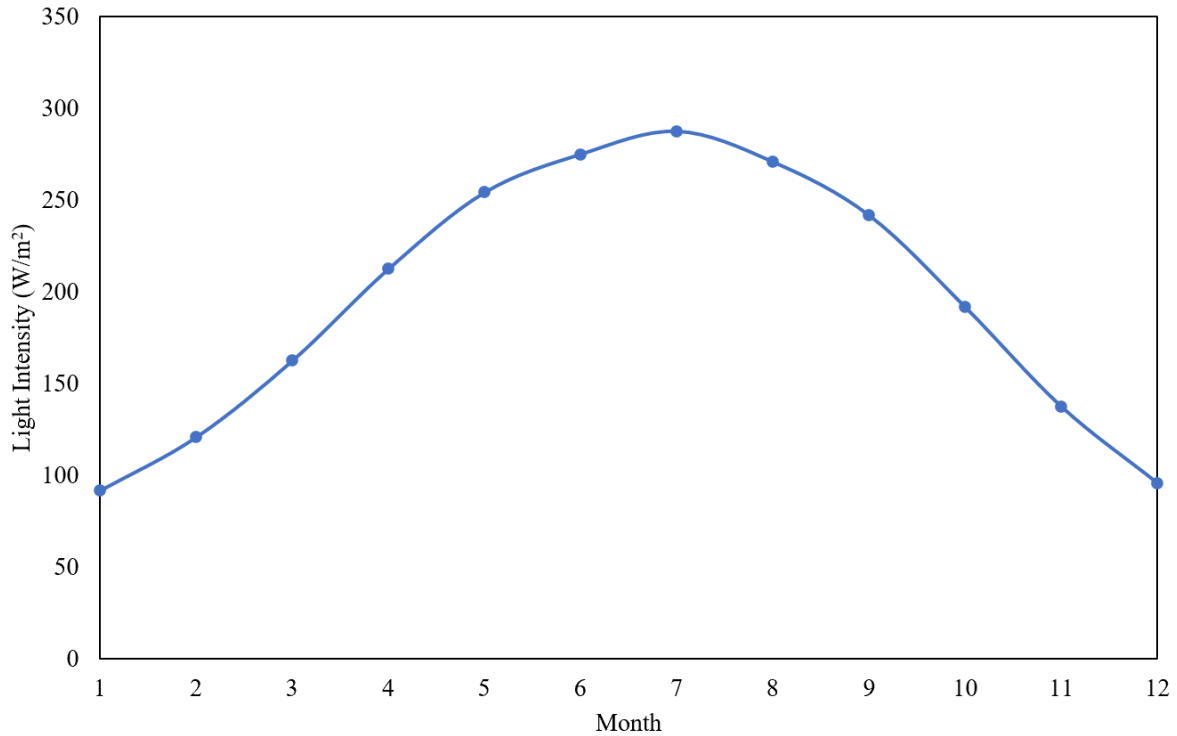


Figure 2-4-02: Average Light Intensity in Harrisonburg, Virginia (Harrisonburg December Weather, Average Temperature (Virginia, United States) - Weather Spark, n.d.)

This suggests that seasonal productivity variation is dependent on temperature rather than light intensity. From the temperature data reported in Figure 2-4-01, the peak productivity of algae production, 100%, will be achieved during June–September, when average temperatures fall in the optimum range. Production is assumed to be at 75% productivity during May and October, and 50% during March, April, and November, and 0% during December, January, and February. This assumption should be tested prior to design.

The pH value of the raceway pond will have an impact on the growth rate of algae, since conditions outside the optimum range will stress the algae out, inhibiting growth (Ru et al., 2020). The optimum pH range for *C. vulgaris* has been reported to be 7.5–8.0 (Rosenberg et al., 2011). Because the raceway ponds will be supplied with carbon source in the form of CO₂ in air, the pH

of the culture will likely be more acidic. However, due to the adaptability of *C. vulgaris* in growing in a wide range of temperatures and light intensity environments (Rosenberg et al., 2011), the algae will be expected to grow at a rate similar to the one found in He et al.

The growth profile of *C. vulgaris* will be assumed to follow the same trend as that shown by *Chlorella sp L1* (He et al., 2016). Further experimentation should be conducted to ensure that *C. vulgaris* will follow a similar growth pattern as *Chlorella sp L1*. As shown in Figure 2-4-03, the dry weight concentration of algae increases from 0.1 g/L to 1.107 g/L in 10 days. Based on this data, the algae will be allowed to grow in the raceway ponds for 10 days from an initial concentration of 0.1 g/L to 1.107 g/L before it is sent to further processing for lipid extraction.

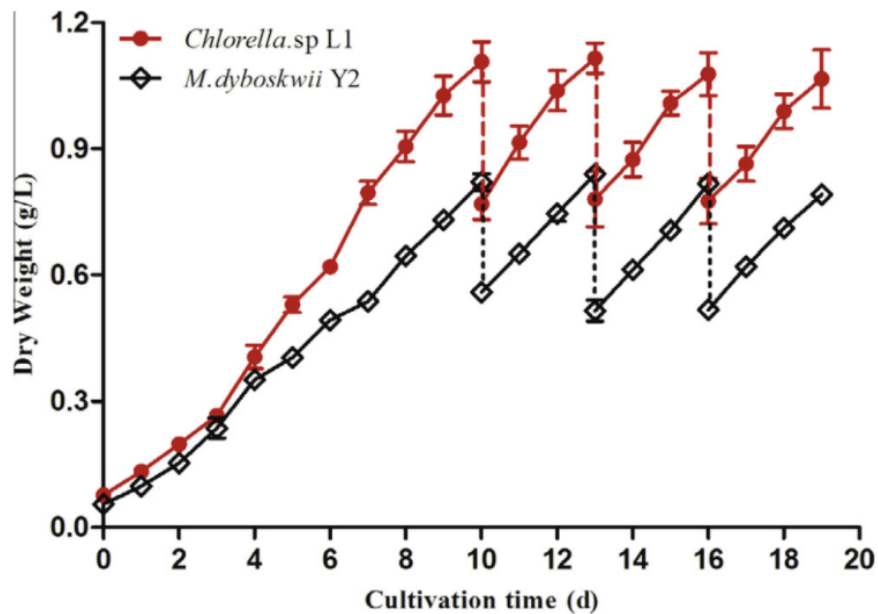


Figure 2-4-03: Growth Profiles of *Chlorella. sp L1* (He et al., 2016)

2.5 Photobioreactor Design Considerations

Initially for the growth of *C. vulgaris*, a hybrid system consisting of a photobioreactor (PBR) and an open-raceway pond was considered. In the hybrid system, growth of algae would be characterized by two distinct phases: a nutrient-rich phase, where algae is allowed to replicate in number (Narala, 2016), and a nutrient-deficient phase, where algae growth rate slows down to induce lipogenesis (Adesanya, 2014). The adoption of a hybrid system for cultivating algae is deemed promising for applications such as biodiesel production, since algae grown with this method have a greater lipid content than just either photobioreactor or raceway pond cultivation (Narala, 2016).

However, after exploring the possibilities of a hybrid system, it was determined that it would be more effective to use only raceway ponds. The reason for this decision was based primarily on two factors: the complexity in the designing of a scaled up PBR and the capital cost of PBR. Due to light penetration being a significant factor for growth in a PBR, scale-up of a PBR is not as simple as making it wider, and due to pressure requirements for aeration of gas through the reactor, it is not as simple as making it longer either. On the other hand, given the lack of scalability, increasing the number of small scale PBR's to fit the capacity given by the plant is not an economically feasible option, either, since PBR's are a large capital investment. Based on the preliminary material balances that were carried out on the photobioreactor cultivation, it was found that in order to supply the growth of algae needed for this process, an estimate for the number of photobioreactors needed was determined. Assuming a flat panel bioreactor composed of 10 panels with dimensions of 1.25 m x 0.5 m x 0.02 m (de Vree et al., 2015), a total of 5,517,600 units of these PBR's would be required. This led to the conclusion that PBR's were not the appropriate choice for this design. Hence, raceway ponds will be used to cultivate the algae.

2.6 Raceway Pond Design Considerations

A turbulent flow is important in raceway design in order to prevent sedimentation, remove oxygen, and increase interaction of algae with sunlight and carbon dioxide (Ali et al., 2018). This velocity and design will lead to a Reynold's number of approximately 187,000, which is well within the turbulent regime, using the following equation (Ali et al., 2018):

$$\text{Re}_h = \frac{\rho_1 D_h U_1}{\mu_1}$$

In this equation, ρ_1 is the density of water, U_1 is the velocity, μ_1 is the viscosity of water, and where D_h is defined as:

$$D_h = \frac{4wh}{w+2h}$$

The power requirement for each raceway was calculated to be 45.4 W, which results in a total power consumption of 2685 kW for all of the raceways, using the equation below (Chisti, 2013):

$$P = \frac{1.59A\rho g U_1^3 f_M^2}{e D_h^{0.33}}$$

In this equation, A can be approximated as the length times the width of the raceway pond, g is gravitational acceleration, e is the efficiency of the motor, drive, and paddlewheel, and f_M is the Manning channel roughness factor. The e value for a paddlewheel located in a channel with a flat bottom is about 0.17, and a f_M of $0.012 \text{ s}\cdot\text{m}^{-1/3}$ was used for the compacted gravel lined with a polymer membrane (Chisti, 2013).

2.7 Dissolved Air Flotation

After cultivation of algae from the raceway ponds, the algae will need to go through an initial de-watering step before the algae lipids can be extracted. A common way this is achieved is with dissolved air flotation (DAF). In the flotation tank of a DAF unit, air is pumped into the cultivated algae medium from the raceway ponds. Small air bubbles form within the algae medium, causing the bubbles to float to the surface and take with it the algae. Using a skimmer, the top layer of the flotation tank will be separated as algae mass, which will now be more concentrated with algae.

One issue with DAF is that it is often paired with the use of flocculants to achieve greater algae and water separation. However, for this design, the dissolved air flotation unit will be optimized to concentrate algae without the use of chemical flocculants. This is because flocculants are expensive (Niaghi et al., 2015) and can be inhibitory to the growth of algae. The latter point becomes more significant when considering that most of the water removed from the DAF unit will be recycled back into the raceway ponds, and will therefore need to be free of chemical flocculants which might impact the growth kinetics of the algae. An optimization study found that DAF units are able to achieve 91% algae separation without the use of chemical flocculants when the incoming algae concentration in water is greater than 500 mg/L (Niaghi et al., 2015). From the design of the raceway ponds and the growth kinetics observed in literature, the incoming stream (1.107 g/L algae in water) will sufficiently exceed the required algae concentration of 500 mg/L.

There are two components to the DAF unit which will specify its design: a saturator tank and a flotation tank. The saturator tank will form air saturated water which will be flown into the flotation tank along with algae slurry sent from the raceway ponds. The flow rate of the saturator tank can be adjusted with a valve, and will have an independent flow rate from the algae inlet flow.

An industrial DAF may resemble the one shown in Figure 2-7-01, where the saturator tank and flotation tank are combined as one equipment.

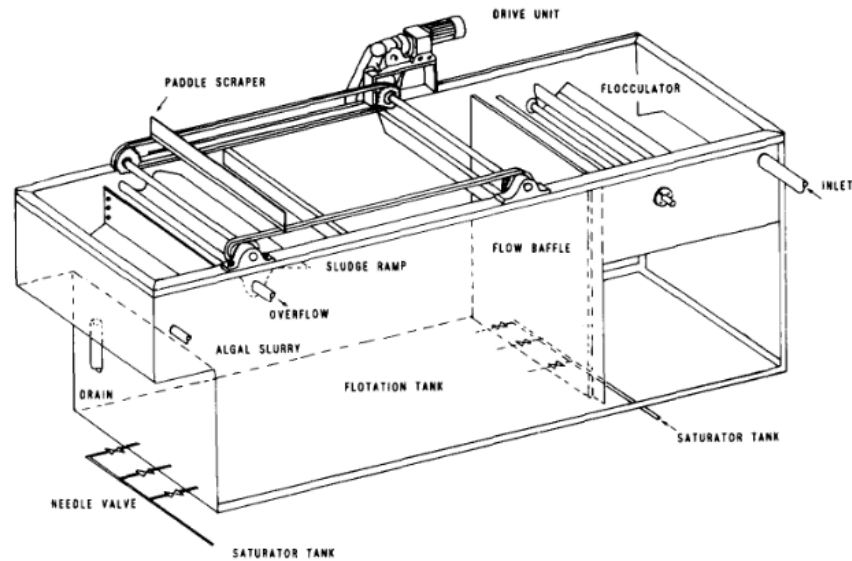


Figure 2-7-01: Industrial scale DAF unit (Sim, 1988)

2.8 Cell Disruption

Following the sludge dewatering step, the algae will go through cell disruption, where the algae cell walls are lysed in order for subsequent lipid extraction steps to achieve greater yield. Studies have found that the lipid recovery improved by a 100-fold when the cells were lysed before solvent extraction than when they were not (Yap et al., 2014). Two different methods for cell disruption were considered.

2.8.1 Acid Disruption

One method for cell disruption that was considered for the process was acid disruption. In this, algae is washed with dilute acid, which helps to dissolve the cell wall and expose intracellular components (Halim et al., 2012). However, it was decided to move away from this method of cell disruption due to the inability to find literature supporting this method of cell disruption at the

scale of this plant; another consideration that led to the pivot away from acid disruption was the recurring cost that would be incurred due to the need for an acid input stream.

2.8.2 High Pressure Homogenization

The cell disruption method which will be used in the process will be high pressure homogenization. High pressure homogenization (HPH) is an industrially preferred method for cell disruption, and many options exist (Gunerken et al., 2015).

For optimal performance, the operating conditions found in Yap et al. were used to model this process to achieve the greatest proportion of lysed cells through the HPH unit. The optimal performance was found when HPH was conducted at 1400 bar, where 80% of cells were lysed (Yap et al., 2014).

2.9 Biomass Drying

2.9.1 Sludge-Dewatering Step

The biomass that is cultivated after DAF will still be water enriched (algae concentration of 7 wt% after DAF). To further dry the algae out and separate water from it, the medium will be sent to a conveyor belt dryer. A conveyor belt dryer discussed by Hosseinizand et al. will be used, which takes in a feed of 25 wt% algae and dries it down to 90 wt% algae. In order to meet the conditions set by Hosseinizand et al., the algae medium post-DAF will need to be initially dried down from 7 wt% to 25 wt% through a sludge-dewatering step. This step will be black-boxed in this process due to project constraints. It is assumed that the entirety of the excess water removed in this step will be recycled back into the raceway ponds.

2.9.2 Conveyor Belt Drying

. To effectively extract the algae for its lipid content, it must be further dried down to its maximum solids concentration of around 90 wt%.

The two main types of drying processes are direct drying, where the material comes into contact with the drying medium, and indirect drying, where the material is dried via a heat transfer surface. As the primary objective of this project is to create an economically viable process for algae biofuel production, the direct drying method of flash drying will be used, where material comes into contact with hot air for a short period of time. This method is cheaper than using indirect methods, and due to the short residence times inside the dryer, product quality is maintained at a high level. This method can also take advantage of using higher solid concentration feeds, further improving economics (Ozer, 2014).

The design of the biomass dryer was modeled based on the equipment used in Hosseinizand et al, where biomass is dried with heated dry air through a conveyor belt dryer. Hosseinizand et al. demonstrated that wet biomass with 25 wt% algae can be dried down to 90 wt% algae, which will be the target water content post-drying. The heated dry air used to dry the biomass enters the conveyor belt dryer at a temperature of 120 °C. In the study, the dry air is brought to this temperature by two sets of heat exchangers: one that uses waste flue gas from a power plant to heat up a thermal fluid (30% v/v ethylene glycol and water), and another that uses the heated thermal fluid to then heat up dry air collected from the atmosphere from 25 °C to 120 °C. As the present design does not use waste flue gas, the dry air will be heated up in a heat exchanger with steam.

2.10 Lipid Extraction using Hexane

Once the lipids have been released from the algae, they need to be extracted from the mixture. The extracted lipids will be used to produce biodiesel later in the process. For ease of modeling, the lipids are assumed to be a mixture of 78 wt% triolein and 22 wt% oleic acid. The structure of triolein is shown by Figure 2-10-01, and the structure of oleic acid is shown by Figure 2-10-02.

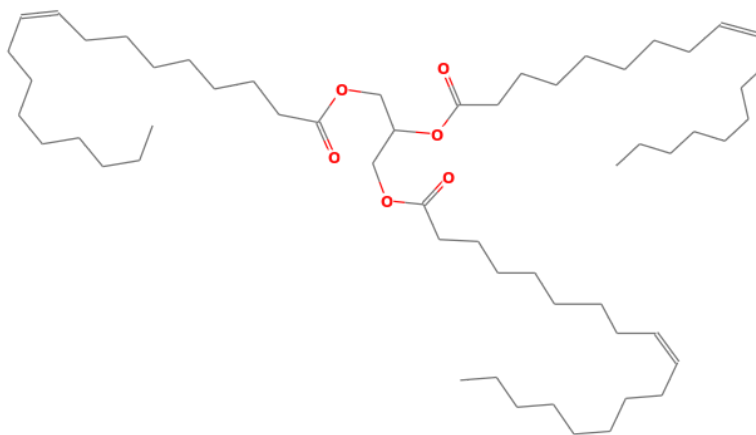


Figure 2-10-01: Structure of Triolein (Rogers & Choudhury, 1978)

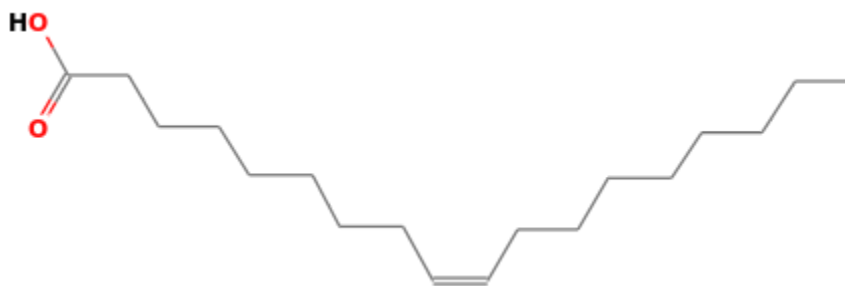


Figure 2-10-02: Structure of Oleic Acid (Rogers et al., 1978)

Triolein and oleic acid are both nonpolar in nature, which allows for them to be separated from the mixture using liquid-liquid extraction. The method of liquid-liquid extraction involves a compound moving from one solvent to another where the two solvents are immiscible with one

another (2.3, 2019). The triolein and oleic acid come into hexane extraction with water as the solvent, which is polar. Hexane will be used as an organic, nonpolar solvent to extract the triolein and oleic acid from the dried algae; hexane was chosen due to it currently being the most economical option for lipid extraction (Patel & Kannan, 2021). In order to ensure there is an excess of hexane in the system, a weight ratio of 30:1 of hexane to lipid will be used for this process. This process is modeled after the conditions discussed by Patel & Kannan, but future work can be done to optimize it so that less hexane is used for extraction, which would likely cut down on material and energy costs.

A horizontal decanter will be used for this separation. It is assumed that the entirety of the lipids present in the system will be recovered due to the large excess of hexane present in the system. The total amount of lipids recoverable in the system will be 37 wt% of the algae biomass, as indicated by studies pertaining to *C. vulgaris* grown in similar conditions (Mujitaba et al., 2012). Once in the decanter, the mixture will be allowed to settle and separate into two distinct layers. The non-polar layer, which consists of lipids and hexanes, will be on the top, and the polar layer, consisting of the rest of the mixture, will be on the bottom. The nonpolar layer will be moved forward in the process for the production of biodiesel. A residence time of 1 hour was estimated for this process. This estimate is based on the residence time for soybean oil, which was found to be 43 minutes (Roque et al., n.d.). Further research and experimentation should be done to determine whether this assumption is appropriate or if it should be amended.

2.11 Hexane Recovery

Once the hexane and lipids exit the decanter, the hexane will need to be separated from the lipids. The hexane will be removed and recycled back into the decanter in order to minimize the

input costs. In order to separate the hexane out of the system, a heat exchanger and flash drum will be used. A flash drum was chosen to separate the hexane from the lipids due the disparity between their volatility. The hexane is much more volatile than the lipids, meaning that it will evaporate at a lower temperature than the lipids. The hexane will then be condensed and recycled back into the decanter used for lipid extraction. The lipids will be cooled to 60°C and sent to acid pre-esterification. Triolein was used to model the lipids in the Aspen Plus software due to difficulties encountered when attempting to simulate oleic acid in the Aspen Plus software.

2.12 Acid Esterification

2.12.1 Esterification Material Balances

From the outlet of the hexane extraction process, around 3,526 kg/hr of algae lipids are produced. These lipids primarily consist of a combination of free fatty acids (FFAs) and triglycerides. In a conventional biodiesel production process, triglycerides undergo a transesterification reaction with the use of an alkali catalyst. However, in lower quality oils, such as the algae lipids used in this process, the presence of FFAs and water can result in undesirable side reactions such as hydrolysis and saponification, reducing the final yield of biodiesel (Suwannakarn, 2009). On top of this, ASTM specifications for biodiesel require acid values beneath 0.05 mg KOH/g, which the crude oil far surpasses (Rahman, 2017). To remedy this, an acid catalyzed esterification step must first occur, where methanol is reacted with FFAs to produce FAMES and water, as shown in Figure 2-12-01.

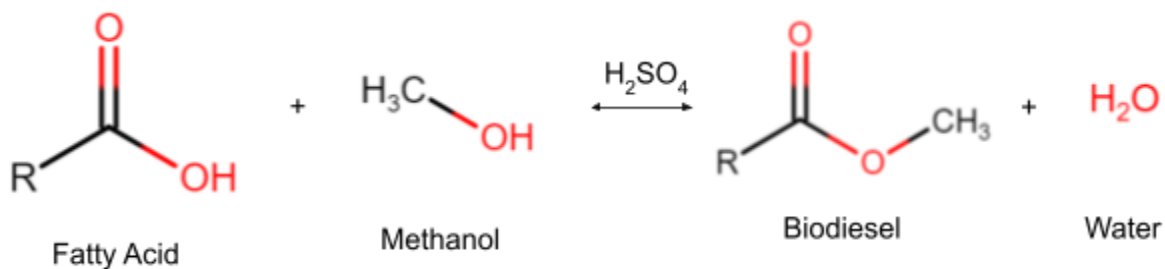


Figure 2-12-01: Acid catalyzed Esterification Reaction

Optimal reaction conditions for minimizing outlet FFA concentration were found to be at a methanol to oil molar ratio of 12:1, and an H₂SO₄ catalyst concentration of 1 wt% (Rahman, 2017). Assuming an average FFA molecular mass of 296 g/mol, the mass of methanol required is 1,614 kg/hr. Because this reaction is running in an excess of methanol, the majority of this methanol stream can be recycled, with any consumed methanol being fed in as a makeup stream. Assuming

that the lipids consist of around 22 wt% FFAs (Suwannakarn, 2009), and that all of the FFAs are reacted, the mass of methanol consumed is 83.96 kg/hr. Because the unreacted methanol is separated from the mixture and recycled back to the reactor, the makeup stream flow rate is equal to the mass of methanol consumed. The required H_2SO_4 concentration is simply 1 wt% of the reaction mixture, and therefore 53.33 kg/hr of 96% H_2SO_4 solution is required.

2.13 Post Esterification Methanol Recovery

2.13.1 Design Specifications and Process Design

Because the acid esterification process is run using excess methanol, the unreacted methanol, along with the acid catalyst and any water produced in the reaction, will need to be removed before the transesterification step. The methanol and acid can then be recycled back to the acid esterification reactor for a more efficient process. To accomplish this, the mixture is first separated into a polar and nonpolar phase using a decanter. The nonpolar phase will contain the triglycerides, FAMEs, and hexane, which are then immediately sent to the base transesterification reactor. The polar phase will contain water, methanol, and sulfuric acid. Before being sent back to the reactor, the methanol and sulfuric acid concentrations must be 99.8 wt% and 96 wt% respectively. Water has a boiling point in between that of methanol and sulfuric acid; as such, any water that was generated during the reaction needs to be removed through a two-step separation process, as outlined in Figure 2-13-01.

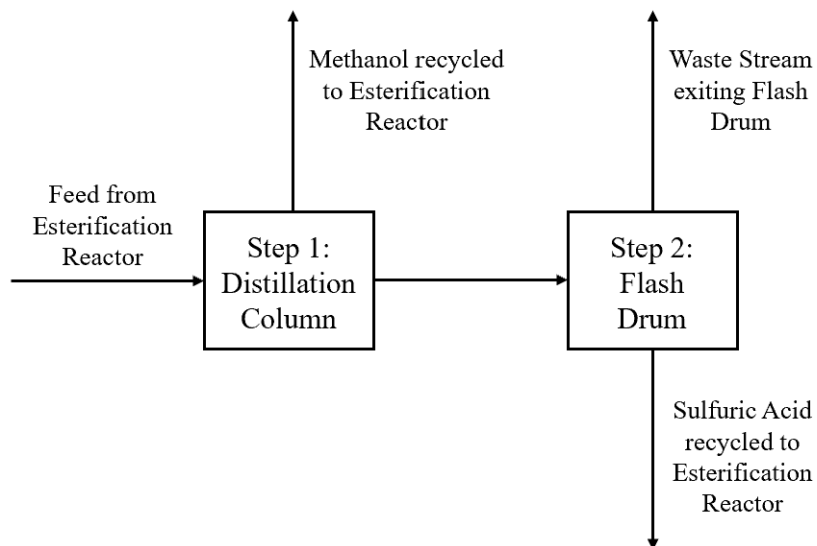


Figure 2-13-01: Block Flow Diagram for Methanol and Acid Recovery

The reaction mixture is first fed into a distillation column, where the methanol is separated out at the top of the column. Optimum values for the reflux ratio, actual number of trays, and feed stage location were calculated using the DSTWU method in Aspen Plus. The bottoms product will consist of diluted sulfuric acid, which will then be concentrated through the use of a heat exchanger and a flash drum. Water will vaporize and be discarded through the top of the drum, while the concentrated acid solution will be collected and recycled back to the reactor.

2.14 Base Transesterification

2.14.1 Trans-Esterification Material Balances

After the acid-esterification reaction produces FAME and water, the product stream will still contain triglycerides that can be converted into FAME. These triglycerides can be converted to FAMES though a base-catalyzed transesterification reaction. This reaction mechanism is shown in Figure 2-14-01. The transesterification reaction will be catalyzed by Potassium Hydroxide (KOH) to undergo the reaction mechanic in Figure 2-14-01.

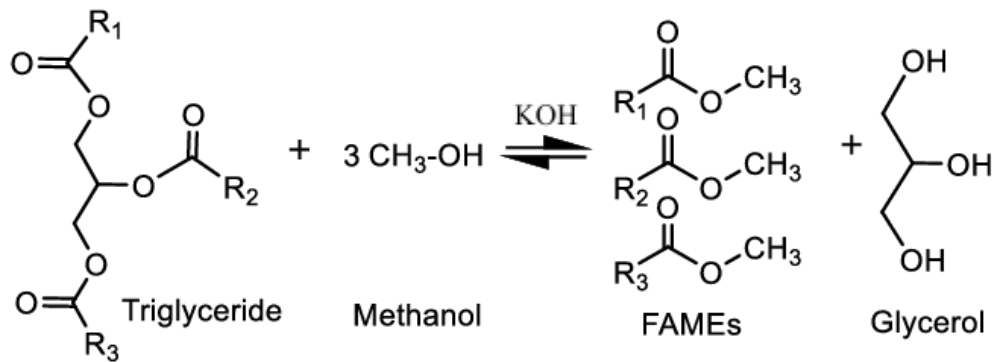


Figure 2-14-01: Transesterification with Base Catalyst (Farobie, 2016 ; Rahman, 2017)

The oil composition of FAMES and Triglycerides in the input stream is 22 and 78 wt% respectively. In total the oil feedstock entering the transesterification reactor is conserved from the esterification process and totalled 2,128 kg/hr of triglycerides and 600.2 kg/hr of FAME. Optimal reaction conditions were found to be at a 9:1 molar ratio of methanol to triglycerides, and 0.75 wt% KOH catalyst. Assuming an average triglyceride molecular weight of 850 g/mol, the required amount of methanol is 721.9 kg/hr, and 26.08 kg/hr of KOH. Like in the acid esterification process, the reaction is run using excess methanol, and the majority of it goes unreacted and is recycled back to the reactor. The required makeup flow rate will be equal to the consumption of methanol plus the amount that is purged from the system, which is equal to 259.92 kg/hr.

2.14.2 Trans-Esterification Reactor Design Considerations

In order to determine the optimal conditions for this reaction, the Rahman study tested various methanol to oil ratios, base catalyst weight compositions, temperatures, and rotations per minute (RPMs). The optimal conditions determined through this study included a 9:1 methanol to oil mole ratio, 0.75 wt% of the base catalyst, 65 °C, 1 atm of pressure, and an impeller speed of 600 RPMs for a 1 L reactor (Rahman, 2017). With all of these conditions in place, biodiesel conversion from trans-esterification peaked at 86.1% after 20 minutes, as shown by Figure 2-14-02 (Rahman, 2017).

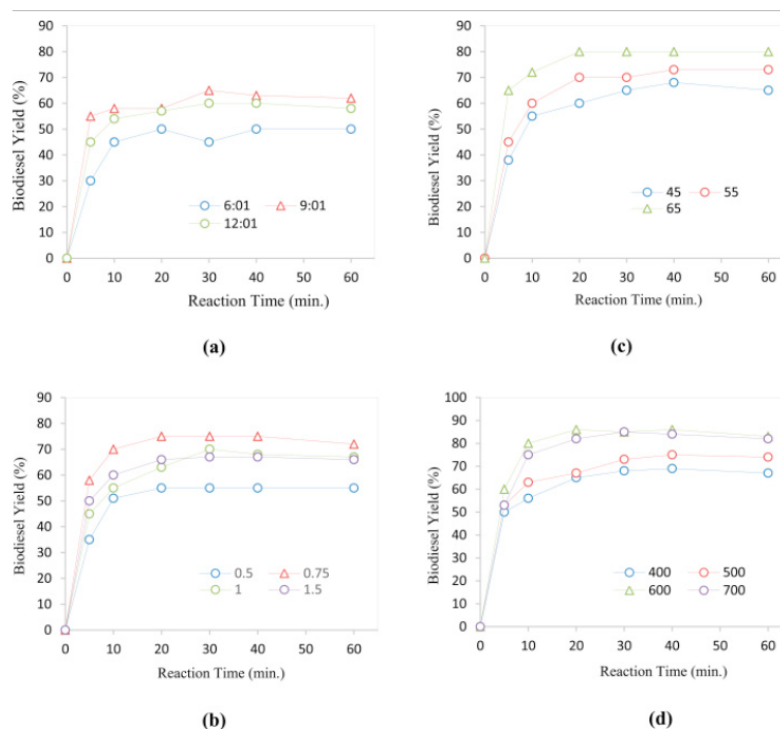


Figure 2-14-02: Sequential Experimentation to Optimize Reactor Conditions

(Rahman, 2017)

The conditions listed out in the optimized trial of the study by Rahman were scaled up for the CSTR and settler used in the large scale process, according to standard configurations.

2.15 Glycerol/Biodiesel Separation

After base transesterification is completed, the contents are first sent to a decanter to separate the polar and non-polar phase. The non-polar phase contains unreacted triglycerides, FAME, and hexane, which are sent to further biodiesel purification steps to derive the main final product, pure biodiesel. The polar phase contains impure glycerol, methanol, and KOH, which are separated further for methanol recovery and glycerol purification to derive the second final product, pure glycerol.

2.16 Post Trans-esterification Methanol Recovery

Similar to the acid esterification reaction, the base transesterification process runs with excess methanol. To design an efficient process that does not require an excessive amount of makeup methanol, the unreacted methanol will need to be recovered from the contents of the base transesterification reactor to be recycled back into the process. The separation of the polar phase (containing impure glycerol, methanol, and KOH) was done through a heat exchanger and a flash separation block, where the top stream was the enriched methanol, which was sent back into the transesterification reactor, and the bottom stream was the glycerol product stream, which was sent for further purification. A purge stream is present in the system before the methanol recycle, and it allows for hexane to exit the system and prevent it from building up. The purge stream removes 5% of the stream's total mass flow. This purge is not economic or optimized, and it could be further improved upon in future work. The NRTL and UNIQUAC methods were used in Aspen Plus to model this process.

2.17 Biodiesel Washing

2.17.1 Biodiesel Specifications and Process Design

The desired product, 100% biodiesel (B100), is subject to several strict specifications by the American Society for Testing and Materials (ASTM), as listed in ASTM D6751. These specifications state that the final biodiesel product must have ≤ 0.05 vol% water, ≤ 0.2 wt% methanol, and ≤ 5 ppm potassium (*Alternative Fuels Data Center: ASTM Biodiesel Specifications*, n.d.). The biodiesel stream leaving the settler after base transesterification will contain trace amounts of both methanol and potassium, failing to meet ASTM specifications. To remedy this, the biodiesel will be first wet washed with water to remove a portion of the polar components (methanol and potassium hydroxide), then dried by distillation to further reduce the water content. The UNIQUAC method was used in Aspen Plus to model this process for all components except for KOH. Figure 2-16-01 shows the relationship between the amount of NaOH in the steam after washing and the amount of water used for washing found by Glisic & Skala. From this figure, it can be shown that 750 kg/hr of water brings the NaOH concentration to around 0.05 wt%. In order to use this data two assumptions were made. Firstly, their research and modeling uses flow rates approximately half of the size present in this project, so the amount of water was doubled to 1,500 kg/hr to account for the scale up. Secondly, it was assumed that KOH would respond in a similar fashion to the water washing as NaOH.

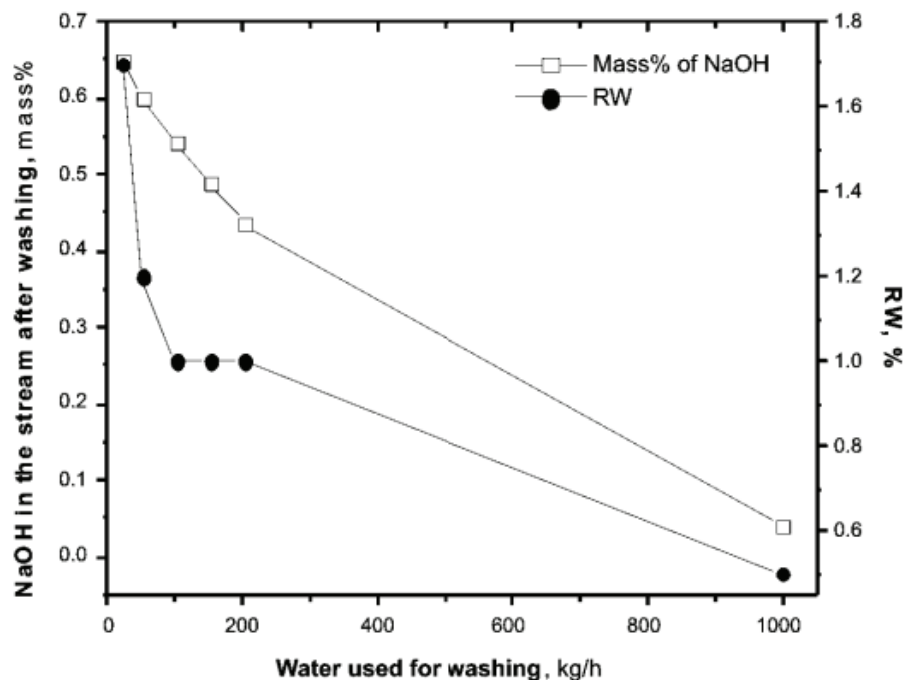


Figure 2-17-01: Amount of NaOH in Feed Stream After Washing (Glisic & Skala, 2009)

2.18 Biodiesel Drying

During the washing process, some of the water used will be entrained in the biodiesel product stream. Because the final product needs to have less than 0.05 vol% water, any entrained water will have to be removed. Water left entrained in the final biodiesel product can lead to unfavorable side reactions as well as fouling the fuel handling systems and damaging tanks and equipment through corrosion (Menges, 2003). The method of water removal will be through distillation, which will bring the biodiesel to compositions that meet the ASTM specifications. The NRTL method was used in Aspen Plus to model this process.

2.19 Neutralization

The Neutralization reaction reaction is taking place to remove the base in the crude glycerol solution that was used for the prior trans-esterification. The Potassium Hydroxide (KOH)

catalyst that enters the column with the crude glycerol will be neutralized by a sulfuric acid solution at a 2:1 base to acid mole ratio. The amount of sulfuric acid required was determined based on the neutralization reaction between KOH and H₂SO₄, outlined in Figure 2-19-01. The reaction will take place in a jacketed T-pipe to increase turbulent flow and promote mixing of the acid base reaction.

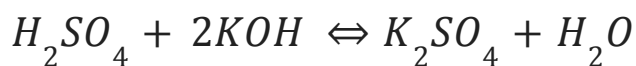


Figure 2-19-01: Neutralization Reaction

2.20 Glycerol Purification

The purpose of filtering the crude glycerol from the neutralization reaction is to rid the product stream from salt and methanol impurities and yield a market-ready product. Refined-grade glycerol is defined by concentrations above 99 wt%. According to the United States Pharmacopeia and Food Chemicals Codex standards, a baseline purity above 99.5% justifies its use in pharmaceutical, cosmetic, food and beverage products (Oliveira, 2022). The membrane separation process is employed to reach the desired weight composition of the crude glycerol byproduct. According to Arrora et al. (2015), the process simulation, economics, and environmental impact are more favorable and profitable for membrane separation than in the alternative vacuum filtration methods. However, a recent study done in response to the 2015 experiment shows that advances in vacuum distillation increase the total flow rate and composition of the glycerol product and will be employed in this system to maximize the byproduct yield (Oliveira, 2022). To perform the separation requires the desired pressure and temperature conditions and after the neutralization the product stream will be sent to a heater, flash separator, a vacuum flash separator, a cooler, a pressure pump, and a heater before it enters the vacuum distillation chamber. This process rids the

crude glycerol of water, methanol, salts and FAME impurities down to negligible amounts. The glycerol purification process was modeled using the ENRTL-RK method in the Aspen Plus software.

2.20.1 Glycerol Vacuum Distillation

Following the removal of salt, water, and methanol, the glycerol vapor leaving the flash column is cooled to enter the liquid phase. The crude glycerol is sent to a vacuum distillation column and the bottom stream leaves as 99.94 wt% product glycerol with a fraction of methanol, water, and FAME impurities remaining.

3. Recommended Design

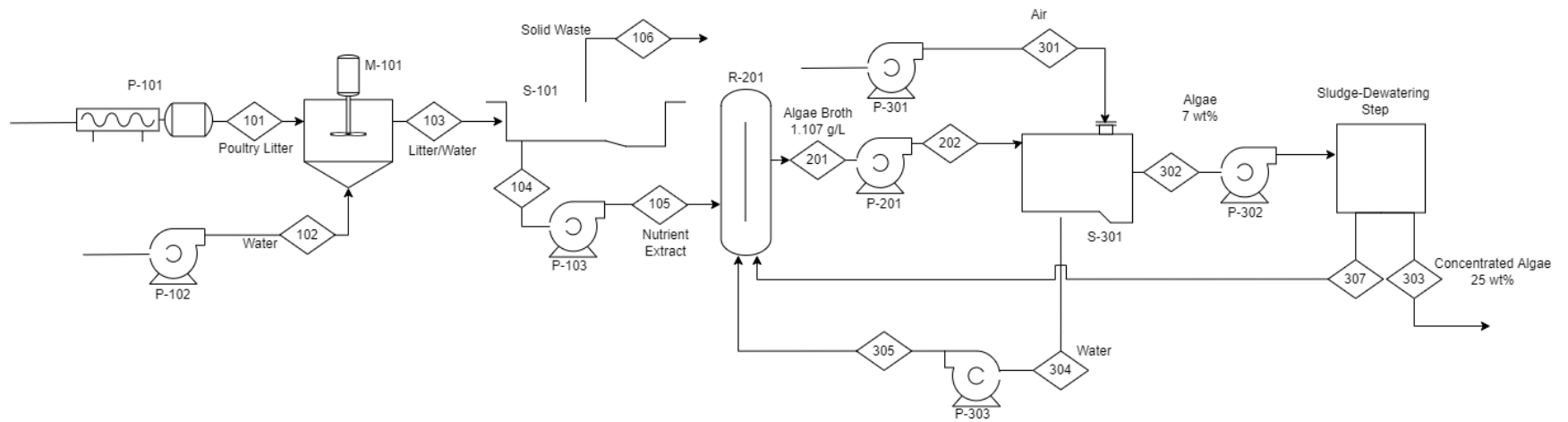


Figure 3-1-01: Nutrient Extraction, Raceway Pond, Dissolved Air Flotation Process Flow Diagram

3.1 Nutrient Extraction

3.1.1 Mixer Design (M-101)

A mixer was designed with dimensions described in Table 3-1-01. The residence time of the mixer was set at 15 minutes, and the dimensions were calculated based on standard configurations for agitating vessels.

Table 3-1-01: Physical Dimensions of Nutrient Mixer

Tank Height (m)	4.2
Tank Diameter (m)	3.8
Impeller Diameter (m)	1.3
RPM	1.8

3.1.2 Settler Design (S-101)

In designing sedimentation tanks, four parameters were identified: tank dimension, surface overflow velocity, residence time, and flow velocity (*Sedimentation Tank Design Parameters*, 2018). The dimensions of each tank are 50 m (L) x 10 m (W) x 5 m (D), for a volume of 2500 m³ each. The surface overflow velocity is described as the volumetric rate of mixture applied into the sedimentation tank per horizontal surface area, which is generally between 12 and 18 m³/day/m² (*Sedimentation Tank Design Parameters*, 2018). The surface overflow velocity in this process will be held at 14.7 m³/day/m². The residence time in the tank is 3.46 hours. The flow velocity describes the velocity at which the mixture travels from the inlet to the outlet in the sedimentation tank, which is usually held at 0.005 m/s (*Sedimentation Tank Design Parameters*, 2018).

The residence times for the mixer and settler is 15 minutes and 3.46 hours, respectively. Based on the relatively short residence time of the mixer, the process schedule will be carried out with one mixer feeding into each of the four settler tanks.

Table 3-1-02: Nutrient Extraction Stream Table

	101	102	103	104	106
Water (kg/hr)	0	27,649	27,649	27,649	0
Litter (kg/hr)	35,784	0	35,784	0	34,233
Nitrogen (kg/hr)	0	0	0	1,150	0
Phosphorus (kg/hr)	0	0	0	401	0
Air (kg/hr)	0	0	0	0	0
Biomass (kg/hr)	0	0	0	0	0
Biomass: Disrupted (kg/hr)	0	0	0	0	0
Hexane (kg/hr)	0	0	0	0	0
Lipids (kg/hr)	0	0	0	0	0

3.2 Raceway Design (R-201)

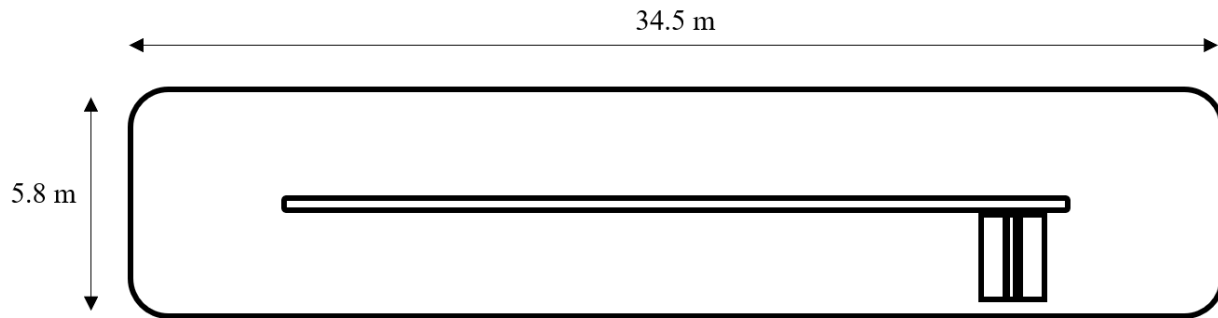


Figure 3-2-01: Raceway Pond Layout

The raceway ponds in this process will be 34.5 m long by 5.8 m wide and the raceways will be 0.4 m tall but only filled to a culture depth of 0.2 m. This design is based off of the design in the study by He et al. The velocity in the raceway ponds will be 0.25 m/s (He et al., 2016).

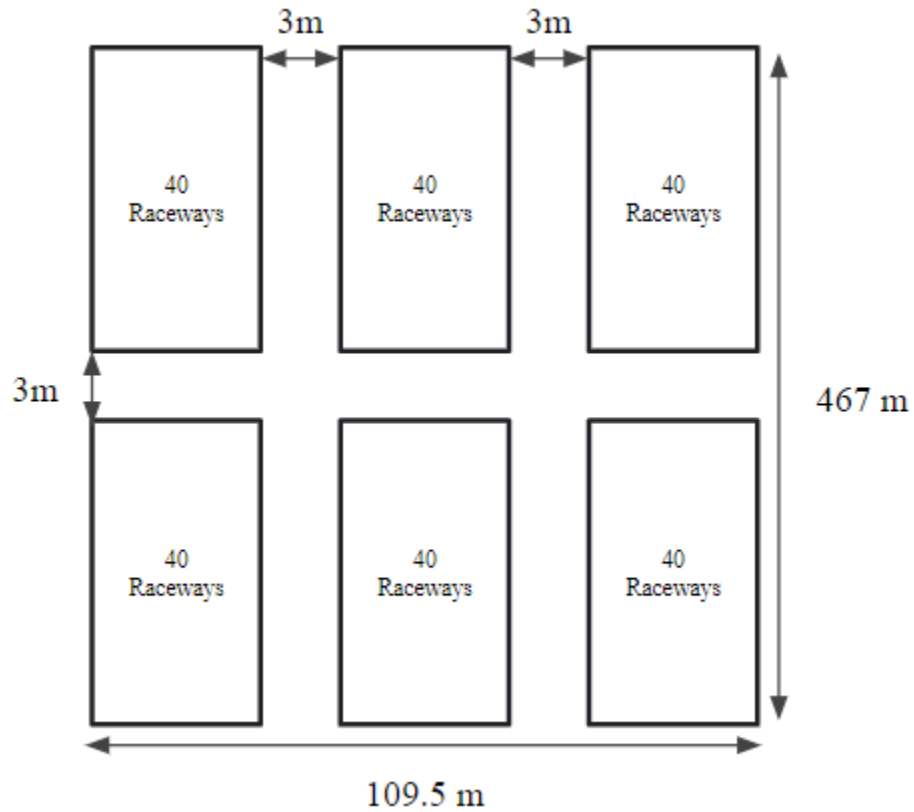


Figure 3-2-02: Configuration of Raceway Ponds

In an attempt to minimize the amount of land required for this plant, the individual raceways described above will be placed together into groups. The raceway ponds will be laid side by side in a fashion that will allow access to each of their shortest sides. There will be 40 raceway ponds in one group. The layout of these groups is shown by Figure 3-2-02. In between each group, there will be 3 m of space to allow for movement and maintenance. A total of 148 groups are needed to provide enough raceway ponds for a batch in this process.

Table 3-2-01: Raceway Pond Stream Table

	105	201	305
Water (kg/hr)	27,649	9,148,818	9,121,169
Litter (kg/hr)	0	0	0
Nitrogen (kg/hr)	1,150	0	0
Phosphorus (kg/hr)	401	0	0
Air (kg/hr)	0	0	0
Biomass (kg/hr)	0	10,128	912
Biomass: Disrupted (kg/hr)	0	0	0
Hexane (kg/hr)	0	0	0
Lipids (kg/hr)	0	0	0

3.3 Dissolved Air Flotation (S-301) & Sludge Dewatering

Most large scale DAF units can accommodate a capacity of around 50 m³ on average, which will be the volume of the flotation tank used in the process.

The operating conditions found in Niaghi et al. will be used in the DAF unit, which outlines the optimized conditions for algae separation without the use of flocculants. The

saturator pressure will be held at 3 atm. The air to solids ratio (A/S ratio), which relates the amount of air passed through the DAF unit and the amount of algae in the inlet slurry, will be held at 0.03. Following the flow rates outlined by Niaghi et al., the flow rate of water saturated with air will be about 1.2 times greater than the flow rate of the inlet algae slurry. Once the saturated water and algae slurry are flown into the DAF unit, the mixture will have a residence time of about an hour, after which algae slurry will be collected off of the surface with a skimmer. Table 3-3-01 describes the material balance around the DAF unit.

Table 3-3-01: DAF Separation & Sludge Dewatering Stream Table

	202	301	302	303	304	307
Water (kg/hr)	9,148,818	0	122,441	27,649	9,026,377	94,792
Litter (kg/hr)	0	0	0	0	0	0
Nitrogen (kg/hr)	0	0	0	0	0	0
Phosphorus (kg/hr)	0	0	0	0	0	0
Air (kg/hr)	0	7,292	0	0	0	0
Biomass (kg/hr)	10,128	0	9,216	9,216	912	0
Biomass: Disrupted (kg/hr)	0	0	0	0	0	0
Hexane (kg/hr)	0	0	0	0	0	0
Lipids (kg/hr)	0	0	0	0	0	0

The inlet algae slurry will have an algae concentration of 1.107 g/L, or 0.1 wt% algae. Post-DAF processing, the overflow collected with the skimmer will have an algae concentration of 75.3 g/L, or 7 wt% algae. One thing to note is that the algae concentration will need to be

further increased from 7 wt% to around 25 wt% in order to meet operating conditions for the cell disruption and biomass drying steps. At this point, however, the step will be black-boxed as a sludge dewatering step, where the algae slurry collected after DAF is further dewatered from a concentration of 75.3 g/L (7 wt%) to 25 wt%.

Based on the daily requirements for algae slurry production capacity described by the values found in Table 3-3-01 and a retention time of 1 hour, the total requirement for DAF units will be 203 units that are each 100 m³ in volume.

It was assumed that the water that was removed in this step was recycled back into the raceway ponds via stream 307.

3.4 Lipid Extraction

The lipid extraction step consists of a high pressure homogenizer M-401 for cell disruption, a conveyor belt dryer E-402 for wet biomass drying, a horizontal decanter S-401 for lipid extraction using hexane, and a flash drum S-402 for hexane recovery.

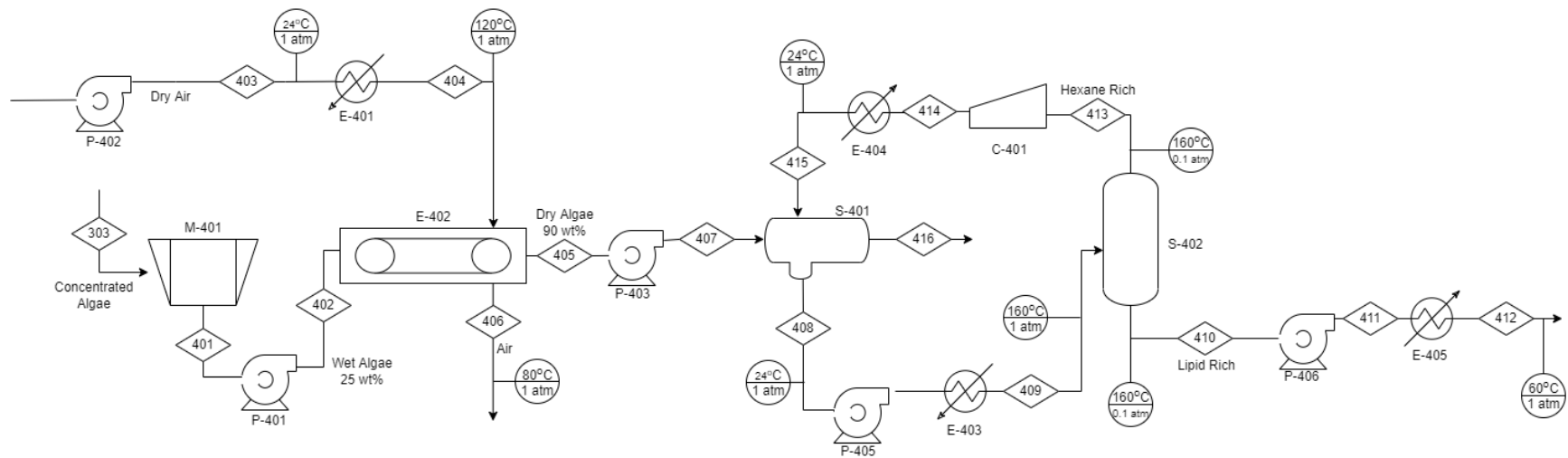


Figure 3-4-1: Lipid Extraction Process Flow Diagram

3.4.1 High Pressure Homogenization (M-401)

Commercial HPH units were available through GEA Italy, which, for a HPH unit that can operate at 1400 bar, will have a maximum flow capacity of about 5,667 L/hr (*Ariete Homogenizer 5400, Powerful, Reliable and Versatile*, n.d.). In order to avoid running at the upper limit, the HPH machines will operate at a flow rate of 5,500 L/hr. Given the capacity of algae slurry to be lysed, the process will require 6 homogenizers.

3.4.2 Biomass Drying (E-402)

By the time the algae slurry is processed through the sludge-dewatering step, the algae concentration in the slurry should be at 25 wt%. The algae slurry will need to be further dried before lipid extraction can be carried out.

The biomass drying process will be modeled after the process outlined by Hosseinizand et al., where the biomass is dried from an algae concentration of 25 wt% to 90 wt%. This will be done in the proposed process by passing hot dry air (120 °C) over the wet algae lined over a conveyor belt. The algae and air exiting the drying unit will both be 80 °C. The dimensions of the conveyor belt will be 32.9 m (L) x 3 m (W), as proposed by Hosseinizand et al. Retention time in the conveyor belt will be 263 minutes.

In order to get the inlet dry air to a temperature of 120 °C, one shell and tube heat exchanger will be used, where steam at 151.9 °C and 5 bars will heat up dry air from 25 to 120 °C. Using Aspen Plus simulations, a heat exchanger with specifications described in Table 3-4-01 was modeled.

Table 3-4-01: Heat Exchanger Specifications for E-401

Overall Heat Transfer Coefficient (W/m ² K)	850
Heat Exchanger Area (m ²)	1,227.9
Heat Duty (kW)	57,392
Inlet Steam Temperature (°C)	151.9
Inlet Steam Vapor Fraction	1
Outlet Steam Temperature (°C)	32.7
Outlet Steam Vapor Fraction	0
Steam Pressure (bar)	5

Table 3-4-02: Homogenization and Drying Stream Table

	303	401	404	405	406
Water (kg/hr)	27,649	27,649	0	819	26,830
Litter (kg/hr)	0	0	0	0	0
Nitrogen (kg/hr)	0	0	0	0	0
Phosphorus (kg/hr)	0	0	0	0	0
Air (kg/hr)	0	0	2,165,865	0	2,165,865
Biomass (kg/hr)	9,216	1,843	0	1,843	0
Biomass: Disrupted (kg/hr)	0	7,373	0	7,373	0
Hexane (kg/hr)	0	0	0	0	0
Lipids (kg/hr)	0	0	0	0	0

3.4.3 Hexane Extraction (S-401)

The decanter used in this process will need a volume of approximately 752 m³. The dried algae stream post-dryer will be mixed in with hexane in the decanter. A residence time of 1 hour was estimated for this process. The contents of the decanter are then sent to hexane recovery (S-402) for hexane and lipid separation.

Table 3-4-03: Hexane Extraction Decanter Stream Table

	407	408	415	416
Water (kg/hr)	819	0	0	819
Litter (kg/hr)	0	0	0	0
Nitrogen (kg/hr)	0	0	0	0
Phosphorus (kg/hr)	0	0	0	0
Air (kg/hr)	0	0	0	0
Biomass (kg/hr)	1,843	0	0	1,843
Biomass: Disrupted (kg/hr)	7,373	0	0	4,645
Hexane (kg/hr)	0	81,841	81,838	0
Lipids (kg/hr)	0	2,728	0	0

3.4.4 Hexane Recovery (S-402)

The lipid-rich stream leaving the decanter will go into a heat exchanger and interface with 300°C steam. The steam going into and the water coming out of the heat exchanger has a flow rate of 37,125 kg/hr and a pressure of 85 atm. The water exiting the heat exchanger has a temperature of 300 °C. The required area calculated by Aspen Plus was 89.51 m². The required heat duty for this heat exchanger design is 14,538 kW. The lipid and hexane rich stream exiting the decanter will exit the heat exchanger at a temperature of 160°C and at a pressure of 1 atm.

The flash process will occur at 160°C and 0.1 atm. The tangent to tangent height of the flash drum is 3.66 m, and its diameter is 5.18 m. The hexane rich stream will come out of the top of the flash drum in the vapor phase, and the lipid rich stream will come out of the bottom of the flash drum in the liquid phase. The mass flow rates of the flash drum's outlet streams and their mass fractions of each component are summarized in Table 3-4-04.

Table 3-4-04: Hexane Flash Separation Stream Table

	409	410	413
Water (kg/hr)	0	0	0
Litter (kg/hr)	0	0	0
Nitrogen (kg/hr)	0	0	0
Phosphorus (kg/hr)	0	0	0
Air (kg/hr)	0	0	0
Biomass (kg/hr)	0	0	0
Biomass: Disrupted (kg/hr)	0	0	0
Hexane (kg/hr)	81,841	2.89	81,838.11
Lipids (kg/hr)	2,728	2,728	0

3.5 Acid Pre-Esterification

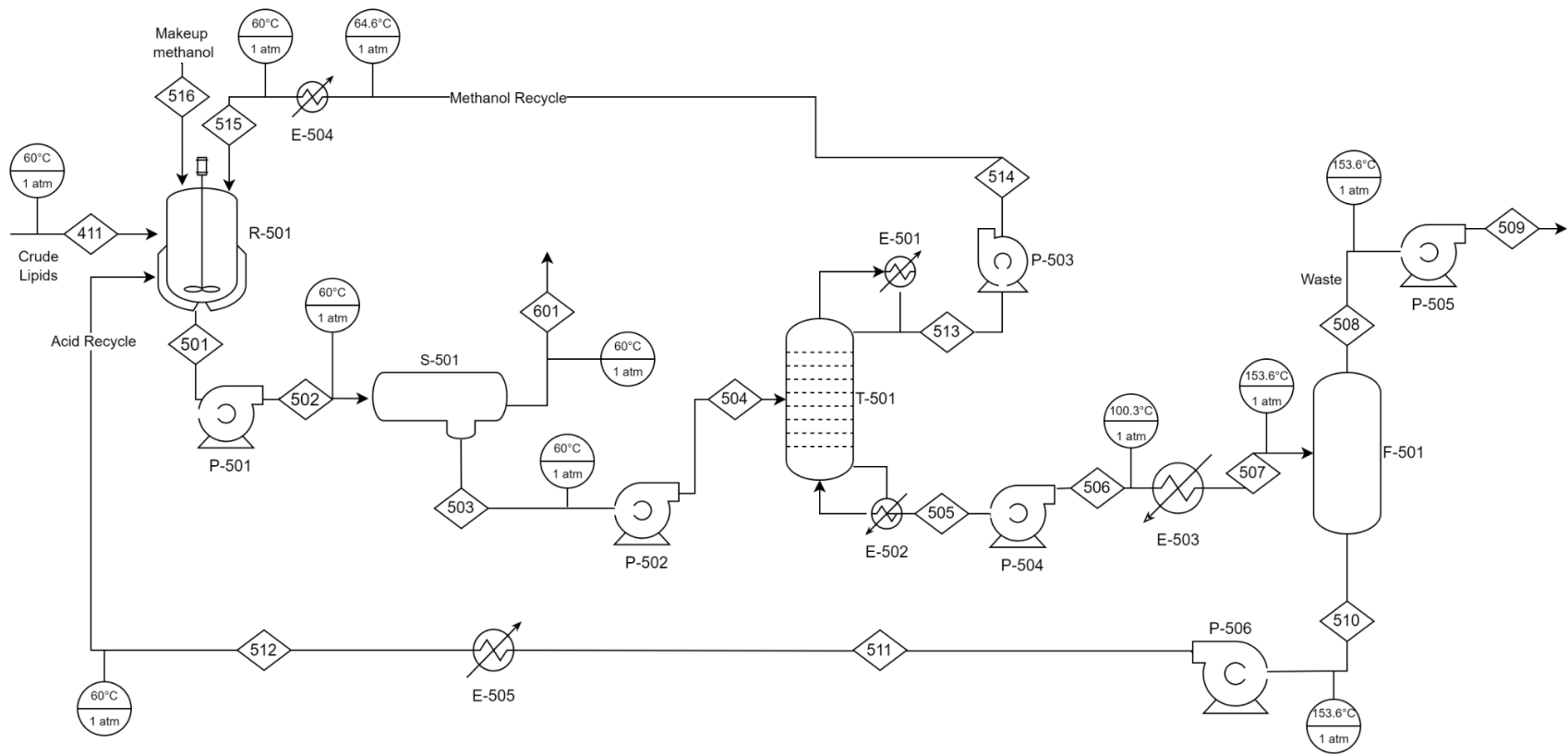


Figure 3-5-01: Acid Pre-Esterification Flow Diagram

The process flow diagram for the acid pre-esterification step is shown in Figure 3-5-01. The process consists of reactor R-501, a two-phase gravity settler S-501, a distillation column T-501, and a flash drum F-501. The compositions of the inlet and outlet streams are summarized in Table 3-5-01.

Table 3-5-01 Acid Reactor Stream Table

	412	501	512	515	516
Methanol (kg/hr)	0	1169	0	1166	11.09
Water (kg/hr)	0	16	1	2	0
H ₂ SO ₄ (kg/hr)	0	39	39	0	0.20
FAME (kg/hr)	0	600	0	0	0
Lipid (kg/hr)	2,128	2,128	0	0	0
FFA (kg/hr)	600	0	0	0	0
Glycerol (kg/hr)	0	0	0	0	0
KOH (kg/hr)	0	0	0	0	0
Hexane (kg/hr)	2.89	2.89	0	0	0
K ⁺ (kg/hr)	0	0	0	0	0
K ₂ SO _{4(s)} (kg/hr)	0	0	0	0	0
HSO ₄ ⁻ (kg/hr)	0	0	0	0	0
SO ₄ ⁻ (kg/hr)	0	0	0	0	0

3.5.1 Acid Reactor (R-501)

Optimal reactor conditions for this process were obtained from literature, and were found to be 60 °C, 1 atm of pressure, a residence time of 90 minutes, and an impeller speed of 400 RPM for a 1 L reaction chamber (Rahman, 2017). Assuming an inlet flow rate of 5,743 L/hr and a residence time of 90 minutes, the required CSTR volume is 8,615 L. Using standard CSTR configurations described in Figure 3-5-02, the required static liquid height and tank diameter were calculated to be 2.22 m. To account for additional head room, a tank height of 2.5 m was chosen. According to the standard configuration, the impeller diameter should be one third of the diameter of the tank, or 0.74 m. The height of the impeller above the bottom of the tank is also 0.74 m. To find the required impeller RPM, the power/volume ratio was held constant from the values obtained from Rahman. Using the scale up equations in Figure 3-5-02, the scaled rotation was calculated to be 53.4 RPM.

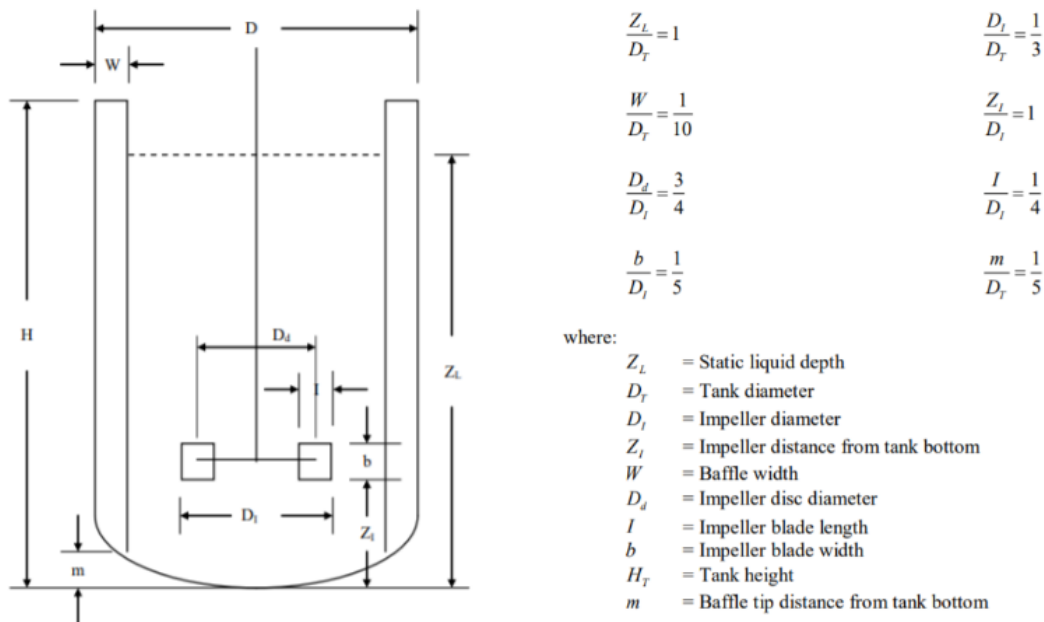


Figure 3-5-02: Scale Up Equations for CSTRs (Trambouze et al., 1988)

3.5.2 Settler (S-501)

This decanter was modeled using Aspen Plus, which calculated key design parameters. Using material flow rates from the reactor, the liquid volume of the settler was calculated to be 3,269 L. The vessel diameter and its tangent to tangent height are 1.07 m and 3.66 m respectively.

Table 3-5-02: Acid Settler Stream Table

	502	503	601
Methanol (kg/hr)	1169	1169	0
Water (kg/hr)	16	16	0
H ₂ SO ₄ (kg/hr)	40	40	0
FAME (kg/hr)	600	0	600
Lipid (kg/hr)	2128	0	2128
Glycerol (kg/hr)	0	0	0
KOH (kg/hr)	0	0	0
Hexane (kg/hr)	2.89	0	2.89
K ⁺ (kg/hr)	0	0	0
K ₂ SO _{4(s)} (kg/hr)	0	0	0
HSO ₄ ⁻ (kg/hr)	0	0	0
SO ₄ ⁻ (kg/hr)	0	0	0

3.5.3 Post-Acid Methanol Recovery Column (T-501)

Values for the reflux ratio, actual number of trays, and feed stage location were found to be 0.468, 45 trays, and above stage 28 respectively. Using these values as a baseline, material and energy balance calculations and sizing was done using the RadFrac method. The column's tangential height was found to be 41.5 m tall, with a tray spacing of 0.6096 m between stages. The diameter was calculated to be 0.762 m. The material stream table for the distillation column is listed above in Table 3-5-03. 99.8% of the methanol in the feed is recovered as the top product, with close to no sulfuric acid entrained.

Table 3-5-03: Acid/Methanol Recovery Distillation Stream Table

	504	505	513
Methanol (kg/hr)	1,169	3	1,166
Water (kg/hr)	16	14	2
H ₂ SO ₄ (kg/hr)	40	40	0
FAME (kg/hr)	0	0	0
Lipid (kg/hr)	0	0	0
Glycerol (kg/hr)	0	0	0
KOH (kg/hr)	0	0	0
Hexane (kg/hr)	0	0	0
K ⁺ (kg/hr)	0	0	0
K ₂ SO _{4(s)} (kg/hr)	0	0	0
HSO ₄ ⁻ (kg/hr)	0	0	0
SO ₄ ⁻ (kg/hr)	0	0	0

The reboiler was calculated to have a heat duty of 531.72 kW. The required surface area of the u-tube reboiler according to Aspen Plus is 8.08 m². The condenser was calculated to have a heat duty of -525.18 kW. The condenser has a required area of 18.4 m² according to Aspen Plus.

3.5.4 Acid Flash Column (F-501)

The bottom stream from the distillation column will be sent to a heat exchanger, where it will interface with a 160°C saturated steam stream. The steam will have a flow rate of 14.25 kg/hr. The acid stream will enter the heat exchanger at 100.3 °C, and exit the heat exchanger at 153.6°C, requiring a heat duty of 9.212 kW. Aspen Plus calculated the required area to be 0.464 m². The drum has a diameter of 0.9144 m and a tangent to tangent height of 3.658 m. Water vapor, along with any residual methanol vapor, will be collected at the top. Concentrated sulfuric acid will be collected at the bottom of the drum at a concentration of 96 wt%, where it will be recycled back to the reactor.

Table 3-5-04: Acid Flash Separation Stream Table

	507	508	510
Methanol (kg/hr)	3	2.83	0.04
Water (kg/hr)	14	11.57	0.51
H ₂ SO ₄ (kg/hr)	40	1.00	39.00
FAME (kg/hr)	0	0	0
Lipid (kg/hr)	0	0	0
Glycerol (kg/hr)	0	0	0
KOH (kg/hr)	0	0	0
Hexane	0	0	0
K ⁺ (kg/hr)	0	0	0
K ₂ SO _{4(s)} (kg/hr)	0	0	0
HSO ₄ ⁻ (kg/hr)	0	0	0
SO ₄ ⁻ (kg/hr)	0	0	0

3.6 Base Trans-Esterification

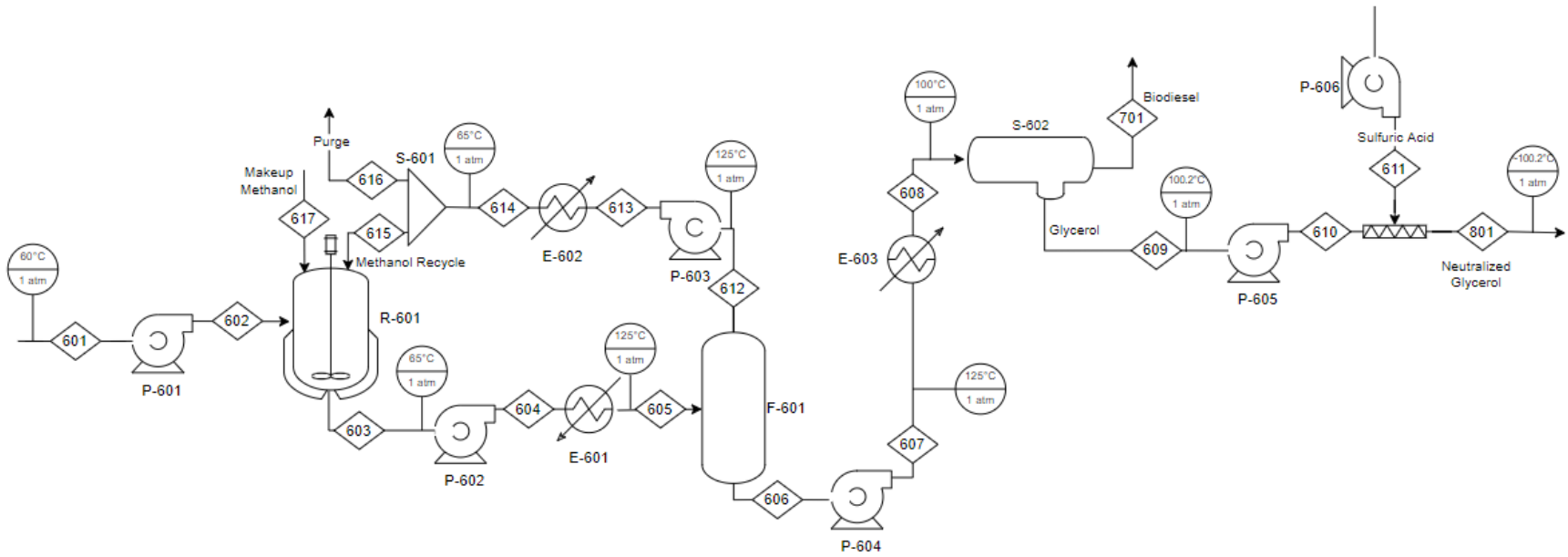


Figure 3-6-01: Base Trans-Esterification Flow Diagram

3.6.1 Base Reactor (R-601)

The required CSTR volume for the Transesterification is 1,453 L when assuming an inlet flow rate of 4,357 L/hr and a residence time of 20 minutes. Using standard CSTR configurations described in Figure 3-5-02, the required static liquid height and tank diameter were calculated to be 1.23 m. To account for additional head room, a tank height of 1.5 m was chosen. Based on the standard configuration, the impeller diameter should be approximately one third of the diameter of the tank, or 0.41 m. A hydrofoil agitator was chosen to be used as the impeller type. The height of the impeller above the bottom of the tank is equal to its diameter, which is 0.41 m. In order to find the impeller's required RPM, the power/volume ratio was held constant from the values obtained from Rahman. Using the scale up equations from Figure 3-5-02, the scaled RPM was calculated to be 116.

Table 3-6-01: Trans-esterification Reactor Stream Table

	602	603	615	617
Methanol (kg/hr)	0	515	462	260
Water (kg/hr)	0	0	0	0
H ₂ SO ₄ (kg/hr)	0	0	0	0
FAME (kg/hr)	600	2,597	0.710	0
Lipid (kg/hr)	2,128	141	0	0
Glycerol (kg/hr)	0	198	1.60	0
KOH (kg/hr)	0	26	0	26
Hexane (kg/hr)	2.89	2.89	2.31	0
K ⁺ (kg/hr)	0	0	0	0
K ₂ SO _{4(s)} (kg/hr)	0	0	0	0
HSO ₄ ⁻ (kg/hr)	0	0	0	0
SO ₄ ⁻ (kg/hr)	0	0	0	0

3.6.2 Methanol Flash Column (F-601)

Like the acid esterification reactor, the base transesterification reactor is operated using excess methanol. This methanol in the reaction mixture needs to be removed before further downstream processing can occur, and can be recycled back into the base reactor. This can be simply done via a flash separation process. The purge stream, 616, in the system before the methanol recycle allows for hexane to exit the system and prevent it from building up. The purge stream removes 5% of the stream's total mass flow. The reaction mixture will enter the heat exchanger at 65°C and exit at 125°C, requiring a heat duty of 267.9 kW. The required heat exchange area was calculated to be 4.43 m² using Aspen Plus. The steam entering the heat

exchanger enters at 200°C and exits at 71°C, and it has a flow rate of 374 kg/hr. The heated mixture is then sent into a flash drum to separate. According to Aspen Plus' calculations, the drum has a diameter of 1.07 m, a tangent to tangent height of 3.66 m, and a volume of 3,269 L.

Table 3-6-02: Trans-esterification Methanol Recovery Stream Table

	605	606	612
Methanol (kg/hr)	515	29	486
Water (kg/hr)	0	0	0
H ₂ SO ₄ (kg/hr)	0	0	0
FAME (kg/hr)	2,597	2,596	1
Lipid (kg/hr)	141	141	0
Glycerol (kg/hr)	198	197	2
KOH (kg/hr)	26	26	0
Hexane (kg/hr)	2.89	0.45	2.44
K ⁺ (kg/hr)	0	0	0
K ₂ SO _{4(s)} (kg/hr)	0	0	0
HSO ₄ ⁻ (kg/hr)	0	0	0
SO ₄ ⁻ (kg/hr)	0	0	0

3.6.3 Settler (S-602)

Because the glycerol produced in the transesterification reaction is immiscible with the FAMES and triglycerides, they can be separated by simply feeding into a decanter. This decanter was modeled using Aspen Plus, which calculated key design parameters using the UNIQUAC method. The volume of the tank should be 2,402 L. The vessel diameter and its tangent to tangent height are 0.914 m and 3.66 m respectively. The stream compositions are shown in Table 3-6-03.

Table 3-6-03: Glycerol/FAME Separation Stream Table

	608	609	701
Methanol (kg/hr)	29	8	21
Water (kg/hr)	0	0	0
H ₂ SO ₄ (kg/hr)	0	0	0
FAME (kg/hr)	2,596	0	2,596
Lipid (kg/hr)	141	0	141
Glycerol (kg/hr)	197	195	2
Hexane (kg/hr)	0.45	0.027	0.423
KOH (kg/hr)	26	6	20
K ⁺ (kg/hr)	0	0	0
K ₂ SO _{4(s)} (kg/hr)	0	0	0
HSO ₄ ⁻ (kg/hr)	0	0	0
SO ₄ ⁻ (kg/hr)	0	0	0

3.7 Biodiesel Purification

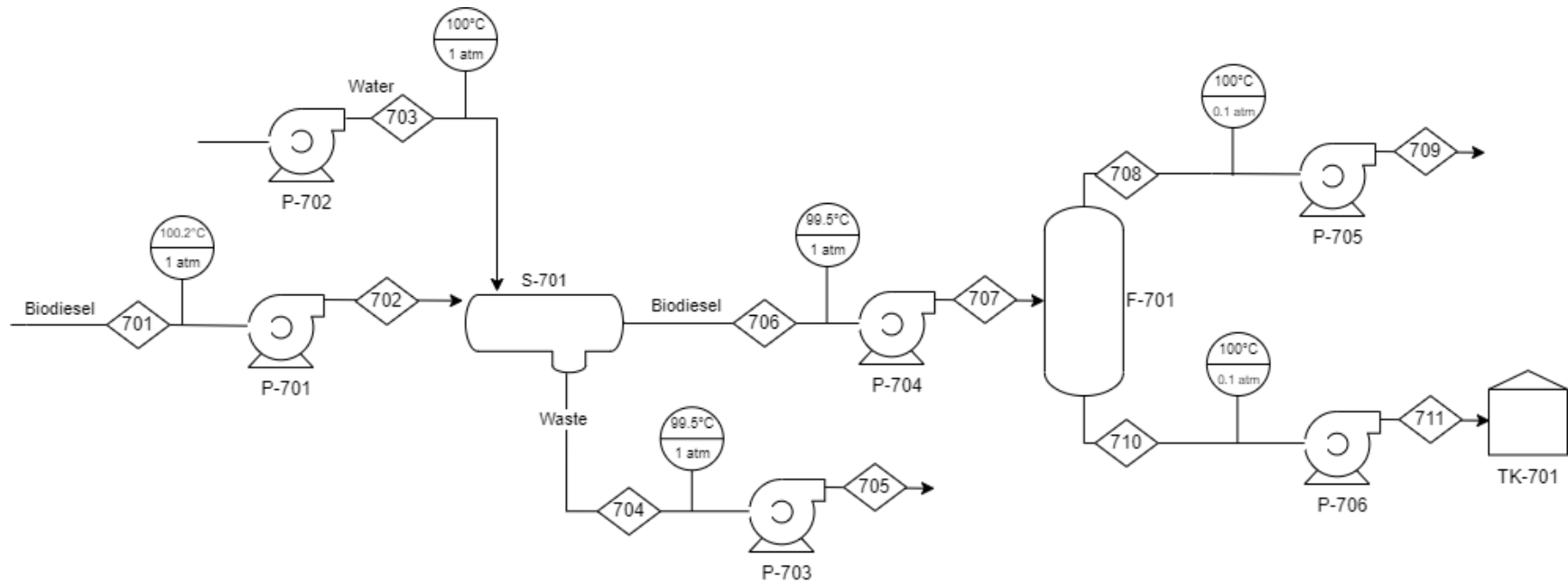


Figure 3-7-01: Biodiesel Purification Flow Diagram

3.7.1 Wet Washing (S-701)

To reduce the amount of potassium in the product, water is sprayed onto the crude FAMES in a decanter. As the water droplets sink in the FAMES, polar impurities such as potassium hydroxide and methanol will be solved into them, eventually settling in the bottom of the tank, where the aqueous layer can be removed. The water stream into the tank has a flow rate of 1,500 kg/hr, at a temperature of 100 °C. According to Aspen Plus' calculations, the decanter has a diameter of 0.914 m, a tangent to tangent height of 3.66 m, and a volume of 2,402 L. The material balance for the biodiesel washing step is important to observe how much of the present impurities are removed from the biodiesel, and it is summarized in Table 3-7-01.

Table 3-7-01: Wet Washing Stream Table

	702	703	704	706
Methanol (kg/hr)	21	0	19	2
Water (kg/hr)	0	1,600	1,583	17
H ₂ SO ₄ (kg/hr)	0	0	0	0
FAME (kg/hr)	2,596	0	0	2,596
Lipid (kg/hr)	141	0	0	141
Glycerol (kg/hr)	2	0	2	0
KOH (kg/hr)	20	0	19	1
Hexane (kg/hr)	0.423	0	0	0.423
K ⁺ (kg/hr)	0	0	0	0
K ₂ SO _{4(s)} (kg/hr)	0	0	0	0
HSO ₄ ⁻ (kg/hr)	0	0	0	0
SO ₄ ⁻ (kg/hr)	0	0	0	0

3.7.3 Biodiesel Drying (F-701)

The flash drum for the biodiesel drying stage will be operated at a temperature of 100°C and a pressure of 0.1 atm. The drum has a volume of 2,402 L. The diameter of the tank and its tangent to tangent height are 0.914 m and 3.66 m respectively. The overall material balance for the biodiesel drying step is summarized in Table 3-7-02.

Table 3-7-02: Biodiesel Drying Stream Table

	707	708	710
Methanol (kg/hr)	2	2	0
Water (kg/hr)	17	16	1
H ₂ SO ₄ (kg/hr)	0	0	0
FAME (kg/hr)	2,596	0	2,596
Lipid (kg/hr)	141	0	141
Glycerol (kg/hr)	0	0	0
KOH (kg/hr)	1	0	1
Hexane (kg/hr)	0.423	0.300	0.123
K ⁺ (kg/hr)	0	0	0
K ₂ SO _{4(s)} (kg/hr)	0	0	0
HSO ₄ ⁻ (kg/hr)	0	0	0
SO ₄ ⁻ (kg/hr)	0	0	0

3.8 Glycerol Purification

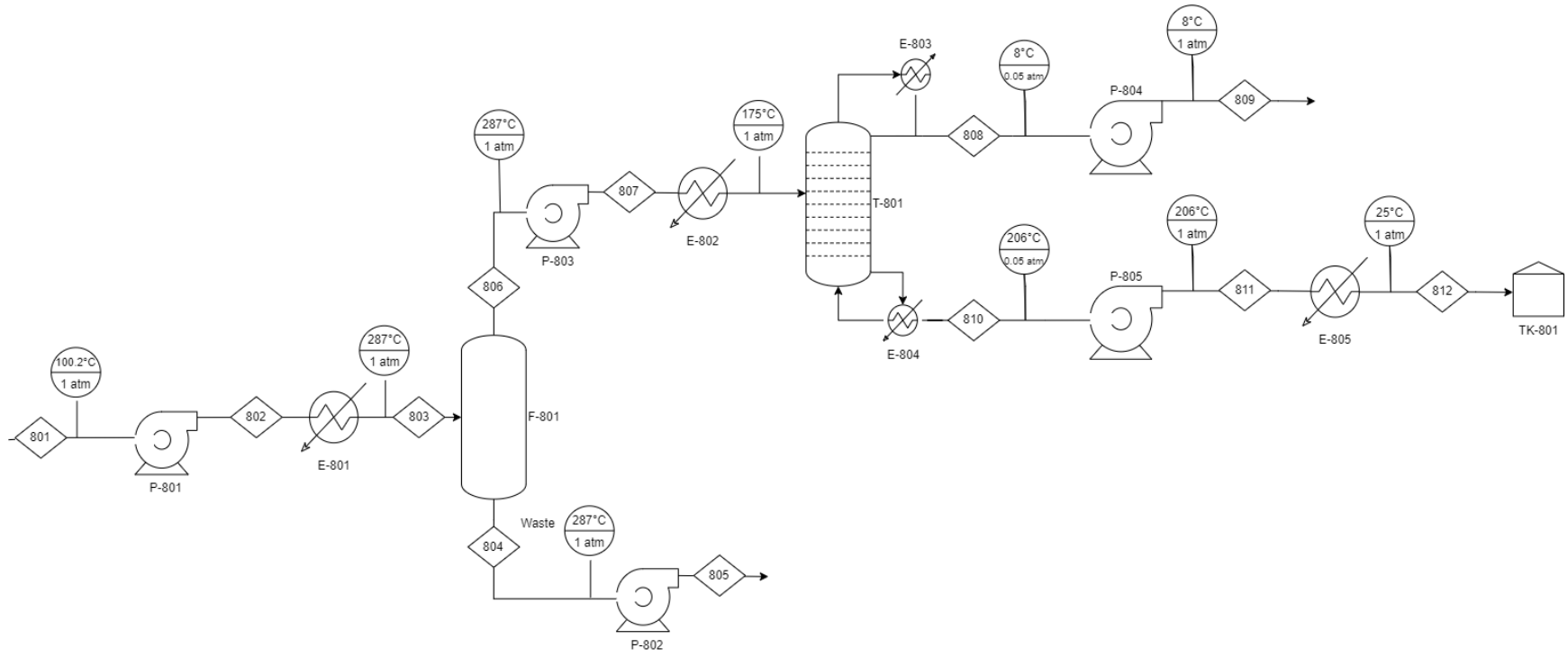


Figure 3-8-01: Glycerol Purification Flow Diagram

3.8.1 Glycerol Neutralization

Table 3-8-01 summarizes the material balance surrounding the neutralization of the glycerol. The flows of streams 605 and 606 will come together using a T-pipe allowing them to mix and react without the need for a vessel.

Table 3-8-01: Glycerol-Acid Neutralization Stream Table

	610	611	801
Methanol (kg/hr)	8	0	8.00
Water (kg/hr)	0	0.25	2.33
H ₂ SO ₄ (kg/hr)	0	5.75	0.06
FAME (kg/hr)	0	0	0
Lipid (kg/hr)	0	0	0
Glycerol (kg/hr)	195	0	195.00
KOH (kg/hr)	6	0	0
Hexane (kg/hr)	0.027	0.027	0.027
K ⁺ (kg/hr)	0	0	0
K ₂ SO _{4(s)} (kg/hr)	0	0	10.10
HSO ₄ ⁻ (kg/hr)	0	0	0
SO ₄ ⁻ (kg/hr)	0	0	0

3.8.2 Glycerol Flash Separation (F-801)

Initially after the neutralization of the glycerol, the salt is removed using a flash column. To accomplish this the liquid solvents, water, methanol, and glycerol are flashed out as vapor following the heating of the reaction mixture to 287.2°C at 1 atm. The heat exchanger used to heat the flash drum's incoming stream has a heat exchanger area of 1.85 m and a heat duty of

62.32 kW. The steam entering the exchanger is at 300°C and 84.9 atm, and it condenses and exits the exchanger at 120.2°C. Table 3-8-02 summarizes the material balance surrounding the glycerol flash separation. . The flash drum succeeds in separating the salt byproduct by maintaining 1 atm and a temperature of 287.2°C. The drum has a volume of 2,402 L. Its diameter and tangent to tangent height are 0.914 m and 3.66 m, respectively.

Table 3-8-02: Glycerol Flash Separation Stream Table

	803	804	806
Methanol (kg/hr)	8	0	8
Water (kg/hr)	2	0	2
H ₂ SO ₄ (kg/hr)	0	0	0
FAME (kg/hr)	0	0	0
Lipid (kg/hr)	0	0	0
Glycerol (kg/hr)	195	6	189
KOH (kg/hr)	0	0	0
Hexane (kg/hr)	0.027	0	0.027
K ⁺ (kg/hr)	1.61	0.13	0
K ₂ SO _{4(s)} (kg/hr)	6.46	9.79	0
HSO ₄ ⁻ (kg/hr)	0.15	0.15	0
SO ₄ ⁻ (kg/hr)	1.92	0.09	0

3.8.3 Glycerol Vacuum Distillation (T-801)

After the removal of salt in the system the majority of the crude glycerol vapor is liquified to send into the vacuum distillation column at 175°C and 1 atm. The heat exchanger used to cool the distillation column's incoming stream has a heat exchanger area of 0.392 m² and a heat duty of -55.62 kW. The cooling water entering the exchanger is at 35°C and 1 atm, and it condenses and exits the exchanger at 100°C. The liquified crude glycerol is sent to the vacuum distillation column which operates at 0.04934 atm with an increasing 0.00009869 atm of pressure as the bottoms product moves down the column. The condenser operates in a partial-vapor-liquid equilibrium, with reflux mass-ratio of 2 and a distillate to feed ratio of 1 mol. The feed enters the column above the fourth tray and both product streams leave as liquid, the distillate at 0.04934 atm and 8.33°C and the bottoms product at 0.05023 atm at 206°C. Table 3-8-03 summarizes the material balance surrounding the vacuum distillation. The column's tangential height was found to be 11.0 m tall, with a tray spacing of 0.6096 m between stages. The diameter was calculated to be 0.457 m. The reboiler was calculated to have a heat duty of 14.15 kW. The required surface area of the u-tube reboiler according to Aspen Plus is 0.472 m². The condenser was calculated to have a heat duty of -13.09 kW. The condenser has a required area of 0.612 m² according to Aspen Plus.

Table 3-8-03: Glycerol Vacuum Distillation Stream Table

	807	808	810
Methanol (kg/hr)	8	8	0
Water (kg/hr)	2	2	0
H ₂ SO ₄ (kg/hr)	0	0	0
FAME (kg/hr)	0	0	0
Lipid (kg/hr)	0	0	0
Glycerol (kg/hr)	189	0	189
Hexane (kg/hr)	0.027	0.027	0
KOH (kg/hr)	0	0	0
K ⁺ (kg/hr)	0	0	0
K ₂ SO _{4(s)} (kg/hr)	0	0	0
HSO ₄ ⁻ (kg/hr)	0	0	0
SO ₄ ⁻ (kg/hr)	0	0	0

3.9 Ancillary Equipment

3.9.1 Pumps and Compressors

Because the majority of the process is at atmospheric pressure, pumps are needed to transport fluids between unit operations. There are a total of 3,832 pumps located throughout the process, with the pump specifications shown below in Table 3-9-01. Asides from P-101, which will be a progressive cavity pump that transports poultry litter into mixer M-101, all pumps will be centrifugal pumps.

Table 3-9-01: Pump Specifications

Equipment	Quantity (Spare)	Flow Rate (m³/day)	ΔP (atm)	Hydraulic Power (kW)	MOC
P-101	1 (1)	1881.2	1	2.21	SS
P-102	1 (1)	665.6	1	0.78	SS
P-103	1 (1)	665.6	1	0.78	SS
P-201	3256 (500)	1488.1	1	1.75	SS
P-301	2 (2)	133857	1	156.98	CS
P-302	1 (1)	665.6	1	0.78	SS
P-303	2 (2)	243640	1	285.73	SS
P-401	1 (1)	665.6	1	0.78	SS
P-402	2 (2)	180000	1	211.09	CS
P-403	1 (1)	146	1	0.17	SS
P-405	1 (1)	3244.66	1	3.81	CS
P-406	1 (1)	82.1091	1.9	0.18	CS
P-501	1 (1)	108.1	1	0.13	SS

Table 3-9-01: Pump Specifications (continued)

Equipment	Quantity (Spare)	Flow Rate (m ³ /day)	ΔP (atm)	Hydraulic Power (kW)	MOC
P-502	1 (1)	38.386	1	0.05	SS
P-503	1 (1)	37.6635	1	0.04	SS
P-504	1 (1)	1.12687	1	0.001	SS
P-505	1 (1)	615.658	1	0.72	SS
P-506	1 (1)	22.8872	1	0.03	SS
P-601	1 (1)	0.364	1	0.0004	CS
P-602	1 (1)	105.043	1	0.12	SS
P-603	1 (1)	11,934.1	1	14.00	SS
P-604	1 (1)	92.9014	1	0.11	SS
P-605	1 (1)	4.07725	1	0.005	SS
P-606	1 (1)	0.08	1	0.0001	SS
P-701	1 (1)	86.6492	1	0.10	SS
P-702	1 (1)	41.8168	1	0.05	SS
P-703	1 (1)	42.0001	1	0.05	SS
P-704	1 (1)	86.8641	1	0.10	SS
P-705	1 (1)	7268.1	1	8.52	SS
P-706	1 (1)	85.9249	1	0.10	SS
P-801	1 (1)	4.33635	1	0.005	SS
P-802	1 (1)	0.253597	1	0.0003	SS
P-803	1 (1)	2645.12	1	3.10	SS
P-804	1 (1)	0.287416	1.95	0.0007	SS
P-805	1 (1)	4.27164	1.95	0.01	CS

All pumps are designed in the same manner, which is by calculating the required hydraulic power. This is done by taking the product of the volumetric flow rate and the differential pressure through the pump. The differential pressure consists of three parts: the actual pressure difference between source and destination operation, frictional losses, and gravity head. An example calculation for pump P-803 is shown below in Table 3-9-02.

Table 3-9-02: Example Specifications Needed for Pump Design

Pump	P-803
Volumetric Flow Rate (m ³ /s)	0.031
Differential Pressure (atm)	1
Hydraulic Power Needed (kW)	3.1

The vast majority of pumps (3,756) are located in the upstream raceway ponds. For each group of 40 raceway ponds, pump P-201 will be placed before and after the pond to allow transport of water to and from the groups. Because there are 1,628 groups of ponds, there will be a total of 3,256 pumps dedicated to water transport due to pumping water in and out of the ponds. There will be an additional 500 pumps kept as spares should any of the pumps fail.

Table 3-9-03: Compressor Specifications

Equipment	Quantity (Spare)	Hydraulic Power (kW)	MOC
C-401	1 (1)	3187.89	CS

3.9.2 Heat Exchangers

A total of 17 heat exchangers are required in this process. Aspen Plus was used to model the heat exchangers in this process. Steam was assumed to be saturated and entering the shell side of every heater. Inlet cooling water was assumed to be at 30°C and on the shell side of every cooler and condenser.

Table 3-9-04: Heat Exchanger Specifications

Equipment	Utility Type	Heat Exchange Area (m²)	MOC
E-401	Steam	1,227.88	CS
E-403	Steam	89.5059	CS
E-404	Cooling water	384.4110	CS
E-405	Cooling water	11.0810	CS
E-501	Cooling water	18.4053	SS
E-502	Steam	8.0826	SS
E-503	Steam	0.4640	SS
E-504	Cooling water	0.8028	SS
E-505	Cooling water	0.0898	SS
E-601	Steam	4.4310	SS
E-602	Cooling water	0.9665	SS
E-603	Cooling water	5.1547	SS
E-801	Steam	1.8550	SS
E-802	Cooling water	0.3925	SS
E-803	Cooling water	0.6123	CS
E-804	Steam	0.4722	CS
E-805	Cooling water	6.2858	CS

3.9.3 Storage Tanks

There are two storage tanks in this process in order to keep the produced products. These tanks were designed to hold 30 days worth of product. Table 3-9-05 shows the size of the two storage tanks. The glycerol storage tank was too small to model as a storage tank, so a 1:1 ratio of diameter and height were used to model it as a vessel.

Table 3-9-05: Storage Tanks

Equipment	Product	Quantity	Size
TK-701	Biodiesel	1	2,200 m ³
TK-801	Glycerol	1	26 m ³

3.10 Batch Operation Schedule

The raceway group's algae will be harvested once every 10 days. There will be one day allotted to the filling and draining of the raceway ponds. Thus, a total of 11 days is required for the cultivation and harvesting of each group of raceway ponds. In order to achieve the maximum production out of a single batch, 148 raceway groups are needed, and in order to maintain a continuous production, 11 batches are needed. As a result, a total of 1,628 groups, or 65,120 raceways are needed for this process.

The plant will operate 9 months of the year due to three months of the year having a temperature that is well below the optimal growth temperature of *Chlorella Vulgaris*. Production is assumed to be at 100% during June through September, 75% productivity during May and October, and 50% during March, April, and November, and 0% during December, January, and February.

4. Economic Considerations

4.1 Total Capital Costs

Equipment costs found in Capcost are calculated based on the average monthly CEPCI value for 2021, which is 708. Some equipment was priced using the Aspen Plus software.

4.1.1 Land

With the layout described in Figure 3-2-02, the total area of the plant for algae harvesting, which includes the raceway ponds and 3 m walkway in between each raceway group, will be 13.9 million m², or 3435 acres of land. An additional 5 acres of land will be dedicated to the placement of other processing equipment, for a total land usage of 3440 acres of land. Land cost per area was determined for cropland value in Virginia for the year 2021 (Ellison, 2021).

Table 4-1-01: Land Cost

Land Usage (acres)	3,440
Cost per area (\$/acres)	4,790
Total Cost (\$)	16,477,600

4.1.2 Nutrient Extraction

The nutrient extraction equipment are the mixing vessel, which is broken up into an impeller and a vessel, and the four sedimentation tanks. The equipment is priced using Capcost.

Table 4-1-02: Nutrient Extraction Equipment

Equipment	Size	MOC	Quantity	Unit Price (\$)	Total Price (\$)
M-101 (Rushton Impeller)	N/A	N/A	1	39,100	39,100
M-101 (Vessel)	47.6 m ³	SS	1	63,600	197,771
S-101 (Sedimentation Tank)	2500 m ³	SS	4	263,000	1,052,000

4.1.3 Algae Cultivation

The total cost to create raceway ponds will be broken up into three parts: the cost to create the ponds, to line the ponds with PVC, and the paddlewheels. The cost of building the raceway ponds was determined by an average price for pond installation (*Learn How Much It Costs to Install a Pond.*, n.d.).

Table 4-1-03: Cost of Creating Ponds

Area for Raceway Ponds (acre)	3435
Area Cost (\$/acre)	3000
Total Cost (\$)	10,305,000

The ponds will be lined with a 2 cm thick layer of PVC liner, which will be used to cover the entire area of the raceway tracks as well as create a median in each raceway. The price of PVC liners was determined via Alibaba (*Alibaba*, n.d.).

Table 4-1-04: Cost of PVC Liner

Volume of PVC needed (m ³)	107,109
Density (kg/m ³)	1.38
Amount of PVC needed (kg)	147,811
Bulk Price of PVC (\$/kg)	1.50
Total Cost (\$)	221,716

Each raceway pond will have a paddlewheel to recirculate algae feed throughout the pond during cultivation. The price of one paddlewheel was determined via Made-In-China (Made-In-China, n.d.).

Table 4-1-05: Cost of Paddlewheel

Unit Price of Paddlewheel (\$/paddlewheel)	100
Total Cost (\$)	6,512,000

The total cost of installing raceway ponds is the sum of the total prices listed in Table 4-1-03, Table 4-1-04, and Table 4-1-05.

Table 4-1-06: Total Cost of Raceway Pond Installation

Equipment	Name	Quantity	Total Cost (\$)
R-201	Raceway Pond	65,120	17,038,716

4.1.4 Dissolved Air Flotation

An industrial scaled DAF unit appropriate for the scale of the process was priced by finding a model sold on Alibaba (Alibaba, n.d.). The proposed process requires 203 DAF units that have an operating capacity of 100 m³. Based on the model specification table given by the supplier, the price of a 100 m³ DAF unit (SS-DAF-150) was assumed to have the price equal to the upper range of the listing.

Table 4-1-07: DAF Unit Model Specification (Alibaba, n.d)

Model	Operating Dimension (m)		
	Length	Width	Height
SS-DAF-150	11.44	3.8	2.5

Table 4-1-08: Cost of DAF Equipment

Equipment	Model	Operating Capacity (m ³)	Quantity	Estimated Price (\$)
S-301	SS-DAF-150	108.7	203	4,060,000

4.1.5 Lipid Extraction

The cost of the GEA Ariete Homogenizer at the specified pressure of 1400 bar was found by scaling the known price of a GEA Ariete Homogenizer at a pressure of 150 bar, using pressure as the primary sizing criterion. The price of the 150 bar homogenizer was found to be 1.75 million Indian rupees (Gea Homogenizer, n.d.), or approximately \$23,000 at the time of writing.

Table 4-1-09: Estimated Price of GEA Ariete Homogenizer

Equipment	Operating Pressure (bar)	Listed Price (\$)	Scaled Price (\$)
Equipment from Gea Homogenizer	150	23,000	N/A
M-401	1400	N/A	88,234

The dryer that will be used in the process is modeled by Hosseinizand et al., with the prices indicated for the capital cost of the dryer. Because the prices are indicated in 2015, the price will need to be scaled according to prices that reflect 2021 using price index scaling. The average monthly CEPCI value in 2015 was found to be 556.8 (*Cepci Index 1950 - 2015*, n.d.).

Table 4-1-10: Scaled Price of Biomass Dryer

Equipment	Year	CEPCI	Scaled Price (\$)
Equipment from Hosseinizand et al.	2015	556.8	712,730
E-402	2021	708	906,273

The vessels used for hexane extraction and subsequent hexane recovery were both priced using Capcost.

Table 4-1-11: Hexane Extraction and Hexane Recovery

Equipment	Size (m³)	MOC	Quantity	Total Price (\$)
S-401	752	CS	1	479,000
S-402	77	CS	1	94,900

4.1.6 Acid Esterification Equipments

The CSTR used for the acid esterification step consists of a tank consisting of SA-615 70 grade carbon steel, and an impeller. The price of the vessel was determined using Capcost. The price of the impeller was determined using INDCO. The price of the post-esterification settler S-501, distillation column T-501, and flash drum F-501 are given by Aspen simulations. The cost of distillation column T-501 includes the cost of the tower, condenser (E-501), reboiler (E-502), and reflux pump. As such, these costs will be omitted when discussing the costs of ancillary equipment.

Table 4-1-12: Cost of Acid Esterification Reactor

Equipment	Size	MOC	Quantity	Total Price (\$)
R-501 (Vessel)	9.68 m ³	SS-316	1	61,354
R-501 (Impeller)	0.74 m	SS-316	1	1,000

Table 4-1-13: Cost of Post-Esterification Separation Equipment

Equipment	Size	MOC	Quantity	Total Price (\$)
S-501	Volume: 3.30 m ³	SS	1	37,700
T-501	<u>Tower</u> Tangent to Tangent Height: 41.5 m Tray spacing: 0.6096 m Diameter: 0.762 m <u>Reboiler</u> Heat duty: 531.72 kW Heat Transfer area: 8.08 m ² <u>Condenser</u> Heat duty: -525.18 kW Heat Transfer area: 18.4 m ²	SS-316	1	1,008,100
F-501	Volume: 2.40 m ³	SS-316	1	33,600

4.1.7 Transesterification Equipments

The base transesterification will also require the use of a CSTR, consisting of a vessel and impeller. The price of the vessel was determined using Capcost. The price of the impeller was determined using INDCO. The price of the post-transesterification separation equipment, which involve flash drum F-601 and settler drum S-601 were determined by Aspen simulations.

Table 4-1-14: Cost of Base Trans-esterification Reactor

Equipment	Size	MOC	Quantity	Total Price (\$)
R-601 (Vessel)	1.78 m ³	SS-316	1	22,939
R-601 (Impeller)	0.41 m	SS-316	1	502

Table 4-1-15: Cost of Post-Trans-esterification Separation Equipment

Equipment	Size	MOC	Quantity	Total Price (\$)
F-601	Diameter: 1.07 m Tangent to Tangent Height: 3.66 m Volume: 3,269 m ³	SS-316	1	37,700
S-601	Diameter: 0.914 m Tangent to Tangent Height: 3.66 m Volume: 2,402 m ³	SS-316	1	33,600

4.1.8 Refinement Equipment

For biodiesel refinement, the equipment are the settler drum S-701, the flash drum F-701, and the storage tank TK-701. The settler drum and flash drum were priced using Aspen simulations, while the storage tank was priced using Capcost.

For glycerol refinement, the equipment are the flash drum F-801, the distillation column T-801, and the storage tank TK-801. The flash drum and distillation column were priced using Aspen simulations, while the storage tank was priced using Capcost. The cost of distillation column T-801 includes the cost of the tower, condenser (E-803), reboiler (E-804), and reflux pump. As such, these costs will be omitted when discussing the costs of ancillary equipment.

Table 4-1-16: Cost of Biodiesel Refinement Equipment

Equipment	Size	MOC	Total Price (\$)
S-701	Diameter: 0.914 m Tangent to Tangent Height: 3.66 m Volume: 2,402 m ³	SS-316	33,600
F-701	Diameter: 0.914 m Tangent to Tangent Height: 3.66 m Volume: 2,402 m ³	SS-316	33,600

Table 4-1-17: Cost of Glycerol Refinement Equipment

Equipment	Size	MOC	Total Price (\$)
F-801	Diameter: 0.914 m Tangent to Tangent Height: 3.66 m Volume: 2,402 m ³	SS-316	34,000
T-801	<u>Tower</u> Tangent to Tangent Height: 11.0 m Tray spacing: 0.6096 m Diameter: 0.457 m <u>Reboiler</u> Heat duty: 14.15 kW Heat Transfer area: 0.472 m ² <u>Condenser</u> Heat duty: -13.09 kW Heat Transfer area: 0.612 m ²	SS-316	106,900

4.1.9 Ancillary Equipment

The cost of pumps were determined with Capcost based on the hydraulic power of each pump. For pumps with required hydraulic power less than the minimum required power necessary to model pumps in Capcost (1 kW), the pumps are standardized to the minimum power.

Table 4-1-18: Cost of Pumps and Compressors

Equipment	Required Hydraulic Power (kW)	MOC/Type	Quantity (Spare)	Total Price (\$)
P-101	2.21	SS/Cavity	1 (1)	33,000
P-102	0.78	SS/Centrifugal	1 (1)	19,928
P-103	0.78	SS/Centrifugal	1 (1)	19,928
P-201	1.75	SS/Centrifugal	3256 (500)	39,359,124
P-301	156.98	CS/Centrifugal	2 (2)	195,864
P-302	0.78	SS/Centrifugal	1 (1)	19,928
P-303	285.73	SS/Centrifugal	2 (2)	456,792
C-401	3187.89	CS/Centrifugal	1 (1)	2,800,000
P-401	0.78	SS/Centrifugal	1 (1)	19,928
P-402	211.09	CS/Centrifugal	2 (2)	244,594
P-403	0.17	SS/Centrifugal	1 (1)	19,928
P-405	3.81	CS/Centrifugal	1 (1)	16,394
P-406	0.18	CS/Centrifugal	1 (1)	13,500
P-501	0.13	SS/Centrifugal	1 (1)	19,928
P-502	0.05	SS/Centrifugal	1 (1)	19,928
P-503	0.04	SS/Centrifugal	1 (1)	19,928
P-504	0.001	SS/Centrifugal	1 (1)	19,928
P-505	0.72	SS/Centrifugal	1 (1)	19,928
P-506	0.03	SS/Centrifugal	1 (1)	19,928
P-601	0.0004	CS/Centrifugal	1 (1)	13,500

Table 4-1-18: Cost of Pumps and Compressors (continued)

Equipment	Required Hydraulic Power (kW)	MOC/Type	Quantity (Spare)	Total Price (\$)
P-602	0.12	SS/Centrifugal	1 (1)	19,928
P-603	14.00	SS/Centrifugal	1 (1)	36,540
P-604	0.11	SS/Centrifugal	1 (1)	19,928
P-605	0.005	SS/Centrifugal	1 (1)	19,928
P-606	0.0001	SS/Centrifugal	1 (1)	19,928
P-701	0.10	SS/Centrifugal	1 (1)	19,928
P-702	0.05	SS/Centrifugal	1 (1)	19,928
P-703	0.05	SS/Centrifugal	1 (1)	19,928
P-704	0.10	SS/Centrifugal	1 (1)	19,928
P-705	8.52	SS/Centrifugal	1 (1)	30,374
P-706	0.10	SS/Centrifugal	1 (1)	19,928
P-801	0.005	SS/Centrifugal	1 (1)	19,928
P-802	0.0003	SS/Centrifugal	1 (1)	19,928
P-803	3.10	SS/Centrifugal	1 (1)	23,064
P-804	0.0007	SS/Centrifugal	1 (1)	19,928
P-805	0.01	CS/Centrifugal	1 (1)	13,500
Total			3832	43,694,590

The cost of heat exchangers were determined using Capcost and Aspen. The results of the calculations are summarized in Table 4-1-19. E-402, E-501, E-502, E-803, and E-804 are not included in this table, as their costs have already been accounted for in previous sections.

Table 4-1-19: Cost of Heat Exchangers

Equipment	Heat Exchange Area (m²)	MOC	Quantity	Price (\$)
E-401	1,227.88	CS	1	187,200
E-403	89.5059	CS	1	54,600
E-404	384.4110	CS	1	102,700
E-405	11.0810	CS	1	27,400
E-503	0.4640	SS	1	10,759
E-504	0.8028	SS	1	10,759
E-505	0.0898	SS	1	10,759
E-601	4.4310	SS	1	15,471
E-602	0.9665	SS	1	10,759
E-603	5.1547	SS	1	15,973
E-801	1.8550	SS	1	15,714
E-802	0.3925	SS	1	10,759
E-805	6.2858	CS	1	6,090
Total			13	420,043

The 2 storage tanks will be priced using Capcost. The biodiesel storage tank, TK-701, will be modeled as a storage tank with Fixed API Roof. The glycerol storage tank, TK-801, will be modeled as a horizontal vessel.

Table 4-1-20: Cost of Storage Tanks

Equipment	Size (m³)	Quantity	Price (\$)
TK-701	2200	1	244,637
TK-801	26	1	33,332
Total			277,969

4.1.10 Working Capital

In order to start production of the plant, a large volume of hexane and methanol must be used in the recycle loop. While most of the hexane and methanol is recovered, the cost of the hexane and methanol needed to “fill up” this recycle loop must be factored into the capital costs of the plant. It was assumed that the volume of each recycle loop would be equivalent to its daily flow rate. These costs are summarized in Table 4-1-21.

Table 4-1-21: Working Capital Costs

Compound (location)	Amount (kg)	Unit Price (\$/kg)	Total Cost (\$)
Hexane (Lipid Extraction)	1,963,627	0.984	1,932,209
Methanol (Acid Esterification)	27,984	0.619	17,322
Methanol (Base Transesterification)	11,664	0.619	7,220
Total			1,956,751

As previously mentioned in Section 2.10, a large quantity of hexane is used for hexane extraction. Optimization of the process can be done by reducing the ratio of hexane to lipids in the extraction step so that the total amount of hexane required for the process is reduced.

4.1.11 Total Capital Costs

Costs listed in the previous sections reflect the cost of the equipment itself. To compute a price that reflects the installation required to place the equipment in the plant, the costs of each relevant piece of equipment will be scaled by a Lang factor of 4. Table 4-1-22 reflects the total cost of capital broken up into sections, including scaled Lang factor costs, where applicable.

Upstream includes nutrient extraction, algae cultivation, dissolved air flotation, and lipid extraction.

Table 4-1-22: Capital Costs Breakdown

Section	Cost (\$)	Lang Factor	Scaled Cost (\$)
Upstream Equipment	24,262,993	4	97,051,972
Acid Esterification & Base Transesterification Equipment	1,236,494	4	4,945,976
Refinement Equipment	175,900	4	703,600
Ancillary Equipment	44,451,502	4	177,806,008
Land	16,477,600	N/A	16,477,600
Working Capital	1,956,751	N/A	1,956,751
Total			297,521,840

4.2 Yearly Operating Costs

4.2.1 Raw Material Costs

Costs for methanol, sulfuric acid, and KOH were sourced from Alibaba (Alibaba, n.d.).

The cost of poultry litter was found to be \$0.0059/kg (Carreira et al., n.d.). The cost of water was assumed to be \$10/1000 gallons (Berry, 2020).

Table 4-2-01: Raw Material Costs

Section	Compound	Amount (kg/day)	Unit Price (\$/kg)	Total Price (\$/day)
Nutrient Extraction	Water	663,570.00	0.0026	1,753
	Poultry Litter	858,810.00	0.0059	5,063
Lipid Extraction	Dry Air			0
	Makeup Hexane	72.00	0.984	71
Acid Esterification	Makeup Methanol	266.16	0.619	165
	H ₂ SO ₄	4.96	0.165	1
Base Transesterification	Makeup Methanol	5637.60	0.619	3,492
	KOH	626.00	0.790	495
	H ₂ SO ₄	134.00	0.165	22

4.2.2 Utility Costs: Electricity

The plant is assumed to be located in Virginia, where the average industrial electricity cost, at the time of writing, was determined to be 6.72 cents per kilowatt-hour. The most significant use of electricity is in the 3,294 pumps located throughout the process. The electricity costs to run these pumps are summarized in Table 4-2-02.

Table 4-2-02: Pumps and Compressors Operating Costs

Equipment	Power (W)	Utility Cost (\$/hr)	Quantity	Total Price (\$/year)
P-101	2206.2	0.15	1	1,299
P-102	780.6	0.05	1	460
P-103	780.6	0.05	1	460
P-201	1745.2	0.12	3256	3,344,974
P-301	156979.9	10.55	2	184,819
P-302	780.6	0.05	1	460
P-303	285727.1	19.20	2	336,399
C-401	3187.9	0.21	1	1,876
P-401	780.6	0.05	1	460
P-402	211093.8	14.19	2	248,530
P-403	171.2	0.01	1	101
P-405	3805.1	0.26	1	2,240
P-406	183.0	0.01	1	108
P-501	126.8	0.01	1	75
P-502	45.0	0.00	1	27
P-503	44.2	0.00	1	26
P-504	1.3	0.00	1	1
P-505	722.0	0.05	1	425
P-506	26.8	0.00	1	16
P-601	0.4	0.00	1	1

Table 4-2-02: Pumps and Compressors Operating Costs (continued)

Equipment	Power (W)	Utility Cost (\$/hr)	Quantity	Total Price (\$/year)
P-602	123.2	0.01	1	73
P-603	13995.6	0.94	1	8,239
P-604	108.9	0.01	1	64
P-605	4.8	0.00	1	3
P-606	0.1	0.00	1	1
P-701	101.6	0.01	1	60
P-702	49.0	0.00	1	29
P-703	49.3	0.00	1	29
P-704	101.9	0.01	1	60
P-705	8523.6	0.57	1	5,018
P-706	100.8	0.01	1	59
P-801	5.1	0.00	1	3
P-802	0.3	0.00	1	1
P-803	3102.0	0.21	1	1,826
P-804	0.7	0.00	1	1
P-805	9.8	0.00	1	6
Total (nonstop production)				4,138,222
Total (production schedule)				2,413,963

The total electricity cost per year was calculated under the assumption of the following production schedule: full capacity for 4 months, 75% capacity for 2 months, and 50% capacity for 3 months, reflecting the seasonal growth rates of *Chlorella vulgaris*. It was also assumed that electricity costs would scale proportionally to the capacity of the plant.

4.2.3 Utility Costs: Steam/Chilled Water

The costs of cooling water, 5 barg low pressure (LP), 10 barg medium pressure (MP), and 41 barg high pressure (HP) steam were obtained from Turton (2018) Table 8.3, and assumed to be \$14.8/1000m³, \$27.70/1000kg, \$29.59/1000kg, and \$29.97/1000kg respectively. The steam/cooling water loads required by each heat exchanger were calculated using Aspen.

Table 4-2-03: Condenser Operating Costs

Equipment	Load (m³/hr)	Utility Cost (\$/hr)	Total Cost (\$/year)
E-404	146.04	2.16	18,933
E-405	0.86	0.01	112
E-501	30.11	0.45	3,904
E-504	0.15	0.00	20.
E-505	0.01	0.00	1
E-602	0.30	0.00	40
E-603	0.07	0.00	9
E-802	0.30	0.00	39
E-803	0.75	0.01	97
E-805	0.10	0.00	13
Total (nonstop production)			23,168
Total (production schedule)			13,515

Table 4-2-04: Heater Operating Costs

Equipment	Steam Pressure	Load (kg/hr)	Utility Cost (\$/hr)	Total Cost (\$/year)
E-401	LP Steam	78,000.00	2,160.00	18,926,856
E-403	HP Steam	37125.00	1,112.64	9,746,694
E-502	LP Steam	897.44	24.86	217,765
E-503	LP Steam	14.25	0.39	3,458
E-601	MP Steam	374.00	11.07	96,944
E-801	HP Steam	93.50	2.80	24,547
E-804	HP Steam	29.73	0.89	7,806
Total (nonstop production)				29,024,070
Total (production schedule)				16,930,707

Like for electricity costs, the total cooling water and steam costs per year were calculated assuming a production schedule that took algae growth conditions into account. The cost of cooling water and steam was also assumed to scale proportionally with the production capacity of the plant.

4.2.4 Labor Costs

Due to the nature of this process, where the plant is distinctly divided between a farm (algae cultivation) and chemical processing (lipid extraction, reaction, and refinement) processes, it is unclear how the labor will be organized. For the simplicity of estimation, the number of operators needed to operate this plant will be estimated by using Equation 8.3 from Turton (2018):

$$N_{OL} = (6.29 + 31.7P^2 + 0.23N_{np})^{0.5}$$

Where N_{OL} is the number of required operators per shift, P is the number of solid-particulate handling steps, and N_{np} is the number of nonparticulate handling steps, which includes every equipment that involves compression, heating and cooling, mixing and reaction. In algae cultivation, each group, which includes 40 raceway ponds, will account for 1 nonparticulate handling step.

Table 4-2-05: Number of Process Steps

	Solid Particulate Steps (P)	Nonparticulate Steps (N_{np})
Upstream	1	1842
Acid Esterification	0	7
Base Transesterification	0	7
Biodiesel Refinement	0	2
Glycerol Refinement	0	5
Storage Tanks	0	2
Total	1	1865

The only solid particulate handling step is the mixer M-101, which mixes poultry litter with water to be sent to the sedimentation tanks S-101 for nutrient extraction. When inputting values for P as 1 and N_{np} as 1865 into Equation 8.3, the number of required operators per shift is 21.6. In order to maintain continuous operation according to the operation schedule, the total number of operators needed for the plant will be scaled by 4.5, giving a total operator count of 97. For every 10 operators, there will be a supervisor required to maintain operations, giving a total supervisor count of 10.

The salaries of the operators were determined based on the average salaries for a chemical plant operator in Virginia (*Chemical Plant Operator I Salary in Virginia | Salary.Com*, n.d.). The salaries of the supervisors were determined to be an average of \$60,000. Insurance for both operators and supervisors were assumed to cost 30% of their respective salaries.

Table 4-2-06: Labor Costs for Operators and Supervisors

	Count	Salary (\$)	Insurance (\$)	Cost (\$/year)
Operators	97	42,596	12,779	5,371,356
Supervisors	10	60,000	18,000	780,000
Total				6,151,356

4.2.5 Operating Costs and Product Revenue

The total operating costs, which includes raw materials, electricity, steam and cooling water usage, and labor costs, are summarized in Table 4-2-07. The product revenue, coming from biodiesel and glycerol, are summarized in Table 4-2-08. Both operating costs and product revenue are summarized on a yearly basis.

Table 4-2-07: Total Yearly Operating Costs

Operating Cost	Cost (\$/year)
Raw Materials	2,323,106
Utility: Electricity	2,413,963
Utility: Steam & Cooling Water	16,944,222
Total	21,681,291

Table 4-2-08: Total Yearly Product Revenue

Product	Wholesale Price	Amount Produced	Revenue (\$/year)
Biodiesel	\$2.50 / gal	4,528,131 gal	11,320,328
Glycerol	\$0.73 / kg	969,359 kg	711,037
Total			12,031,365

4.2.6 Taxes and Other Fees

For simplicity, the property tax rate of the farmland required for this process is assumed to be equal to the current average property tax rate in Rockingham County Virginia, which is \$0.74/\$100 of assessed value per year (*Tax Rates | Rockingham County, VA - Official Website*, n.d.). This results in an annual cost of \$121,934 in taxes assuming \$16,477,600 worth of land usage.

Depreciation was calculated using the straight-line method as described in Turton (2018), under the assumption that the total capital cost of the plant has a class life of 9.5 years, and has a salvage value of 0. Under these assumptions, there is an annual depreciation of \$22,629,560. To calculate the income tax, the depreciation is subtracted from the total operating profit before the tax rate is applied. Income tax is assumed to be at a rate of 27%, combining federal and Virginia corporate income tax rates (*How Does the Corporate Income Tax Work?*, n.d.; *Virginia State Income Tax*, n.d.). Under the assumption that diesel prices are \$2.50/gallon and glycerol prices are \$0.33/lb, the operating cash flow is negative, so no income tax is subtracted.

4.3 Cash Flow Analysis

The overall cash flow per year is summarized in Table 4-3-01.

Table 4-3-01: Operating Cash Flow

Item	Cash Flow (\$/yr)
Plant Operation Costs	-21,681,291
Labor	-6,151,356
Revenue	12,031,365
Property Tax	-121,934
Income Tax	0
Total	-15,923,216

The total lifespan of the plant is assumed to be 22 years. This includes 18 months of plant construction, and 6 months of plant startup. The plant will run for 20 years assuming the cash flow calculated in Table 4-3-01, after which it will be deconstructed. The plant and all of its equipment is assumed to have no salvage value, but the land value and working capital can be recovered for \$16,477,600 and \$1,956,751 respectively. The cumulative discounted cash flow is calculated with a discount rate of 0.1. The internal rate of return was calculated to be -10.3%.

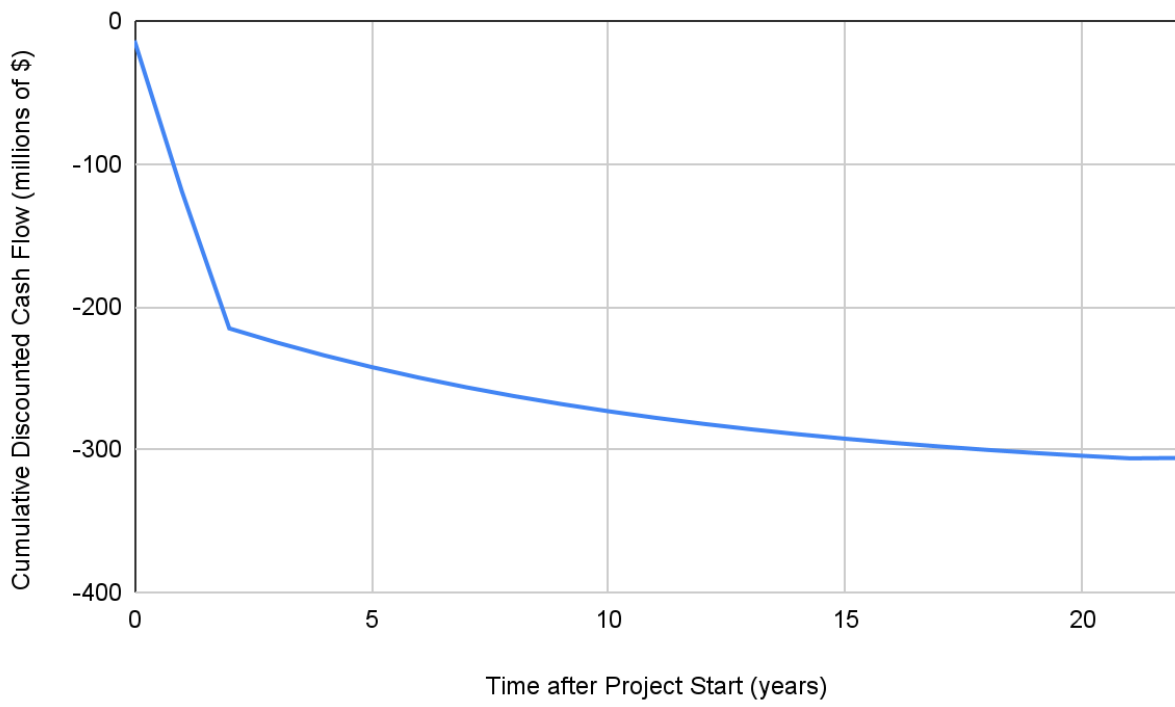


Figure 4-3-01: Cumulative Discounted Cash Flow Diagram

4.4 Scenarios

4.4.1 Increased Diesel Price

The first scenario operates under the assumption that diesel prices will be \$14.25/gallon, as opposed to the \$2.50/gallon assumed for the cash flow analysis. This could potentially occur as a result of a government subsidy of biofuel, or simply due to supply and demand fluctuations as a result of societal factors. The only change to the economics expected with this scenario is an increase in the yearly product revenue.

Table 4-4-01: Total Yearly Product Revenue (Higher Biodiesel Price)

Product	Wholesale Price	Amount Produced	Revenue (\$/year)
Biodiesel	\$14.25 / gal	4,528,131 gal	64,525,867
Glycerol	\$0.73 / kg	969,359 kg	711,037
Total			65,236,904

Table 4-4-02: Operating Cash Flow (Higher Biodiesel Price)

Item	Cash Flow (\$/yr)
Plant Operation Costs	-21,681,291
Labor	-6,151,356
Revenue	65,236,904
Property Tax	-121,934
Income Tax	-10,066,227
Total	27,216,096

Under these assumptions, the plant now generates a post-tax profit of \$27,216,096 per year. The cumulative discounted cash flow diagram is shown in Figure 4-4-01, which again

assumes a discount rate of 0.1, and that the land value and working capital can be recovered for \$16,477,600 and \$1,956,751 respectively.

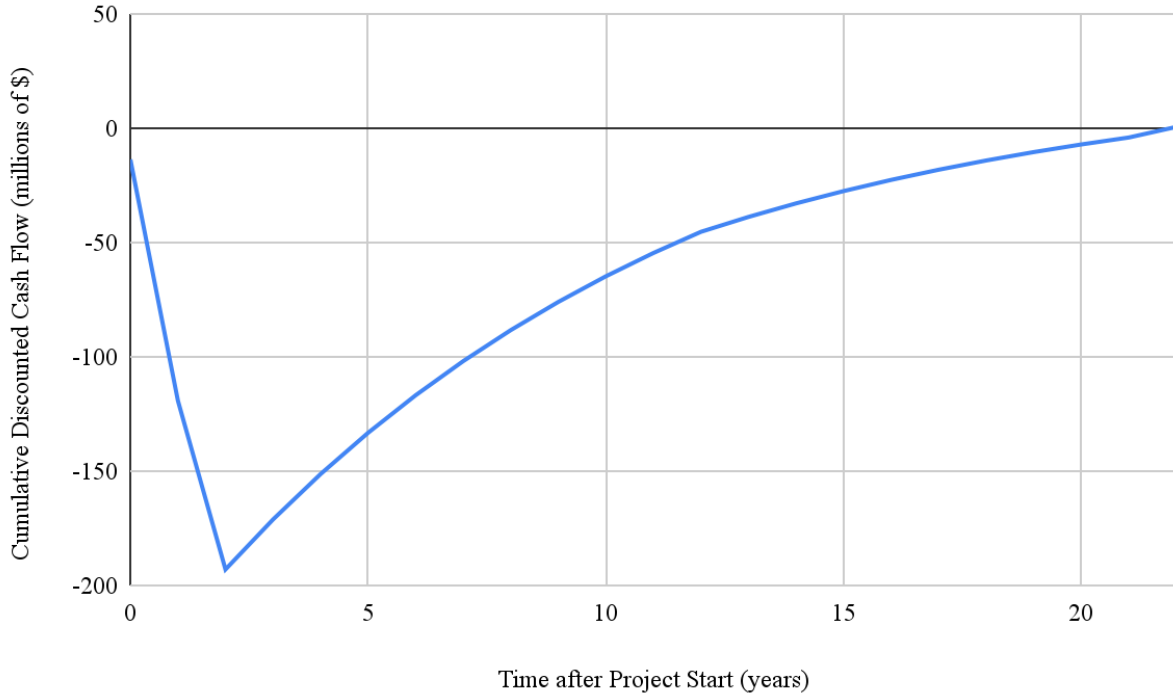


Figure 4-4-01: Cumulative Discounted Cash Flow Diagram (Higher Biodiesel Price)

Under these conditions, the project will just barely break even, with a cumulative discounted cash flow of \$632,800 at decommissioning. While these conditions could potentially be met with a combination of government subsidies and elevated gas prices akin to those seen in Europe (*Diesel Prices around the World, 11-Apr-2022, n.d.*), the return on investment is still not enough to justify the project in its current state.

4.4.2 Free Poultry Litter

The second scenario assumes the use of free poultry litter, through either direct association with poultry farmers, or through government subsidies. The only change to the economics expected with this scenario is a reduction in the operational costs. The amount reduced will be equivalent to the yearly cost of poultry litter in raw materials.

Table 4-4-03: Yearly Operating Costs (Free Poultry Litter)

Operating Cost	Cost (\$/year)
Raw Materials	891,655
Utility: Electricity	2,413,963
Utility: Steam & Cooling Water	16,944,222
Total	20,249,840

Although yearly operation costs are reduced by around 6.6%, the operating cash flow is negative, assuming that the revenue is generated by selling biodiesel at \$2.50/gallon and glycerol at \$0.33/lb. Therefore, no income tax will be subtracted.

Table 4-4-04: Operating Cash Flow (Free Poultry Litter)

Item	Cash Flow (\$/yr)
Plant Operation Costs	-20,249,840
Labor	-6,151,356
Revenue	12,031,365
Property Tax	-121,934
Income Tax	0
Total	-14,491,765

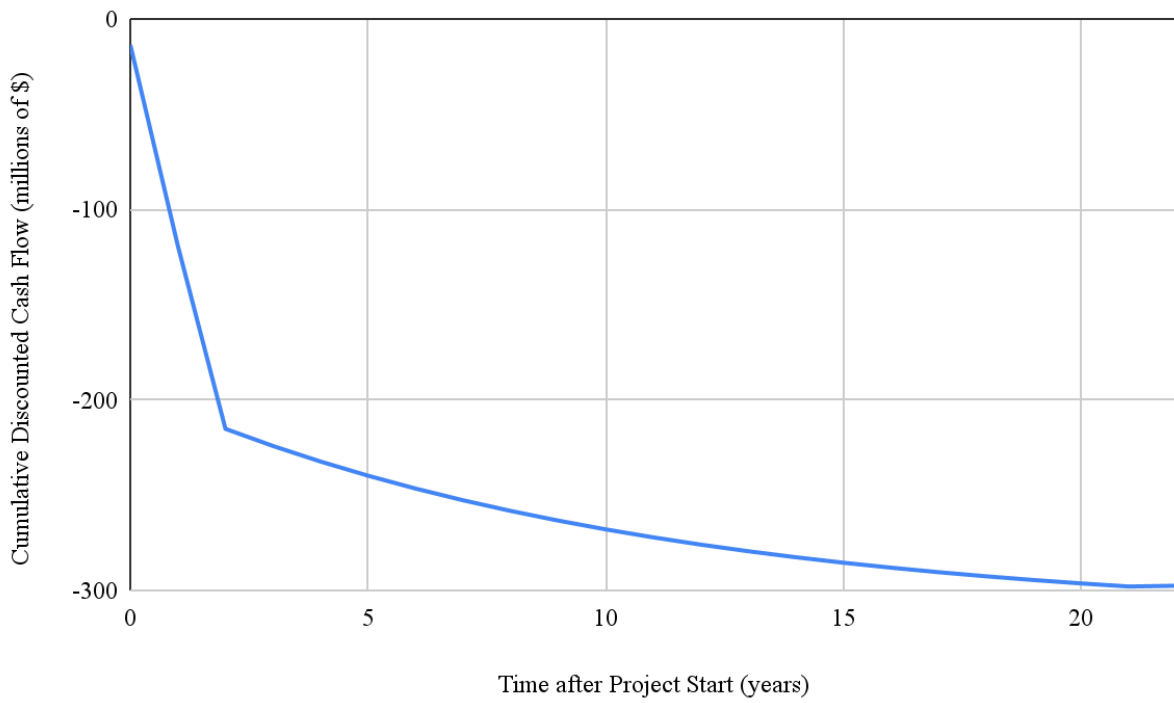


Figure 4-4-02: Cumulative Discounted Cash Flow Diagram (Free Poultry Litter)

4.4.3 Eliminate Glycerol Refinement

The third scenario assumes that, rather than purifying the glycerol byproduct generated during transesterification, the glycerol is simply disposed of as an additional waste stream. This would mean that biodiesel will be the only source of revenue, however, several costs will be reduced as a result.

All capital equipment involved in the glycerol refinement steps will be eliminated, which also may affect the number of operators needed and reduce labor costs as well. Several methods for handling crude glycerol disposal exist. One is through combustion, which is a widely used method, though not an economically favorable one (Farm-Energy). For that reason, crude glycerol will be sold to larger refineries which will purify the glycerol further. Crude glycerol can be sold for 5 cents/lb (Farm-Energy). A summary of how the labor, operating cost, capital, and cash flow change through this alternate scenario. Land capital and working capital will be the same as the base scenario, as the glycerol refinement steps only account for a fraction of the required equipment and no working capital.

Table 4-4-05: Capital Saved from Eliminating Glycerol Refinement Process

Equipments Saved	Pumps Saved	Capital Saved (\$)	New Total Capital (\$)
5 (E-801, E-802, E-805, F-801, T-801)	6 (P-606, P-801, P-802, P-803, P-804, P-805)	1,079,244	296,442,596

Table 4-4-06: Labor Requirement (No Glycerol Refinement)

	Operators	Supervisors
Number Required (Base)	97	10
Number Required (Scenario 3)	97	10

Table 4-4-07: Total Operating Cost (No Glycerol Refinement)

Base Operating Cost (\$)	21,681,291
Electricity Savings (\$)	-1,835
Steam/CW Savings (\$)	-32,502
Total Operating Cost (\$)	21,646,954

Table 4-4-08: Total Yearly Product Revenue (No Glycerol Refinement)

Product	Wholesale Price	Amount Produced	Revenue (\$/year)
Biodiesel	\$2.50 / gal	4,528,131 gal	11,320,328
Glycerol	\$0.11 / kg	1,073,424 kg	118,325
Total			11,438,653

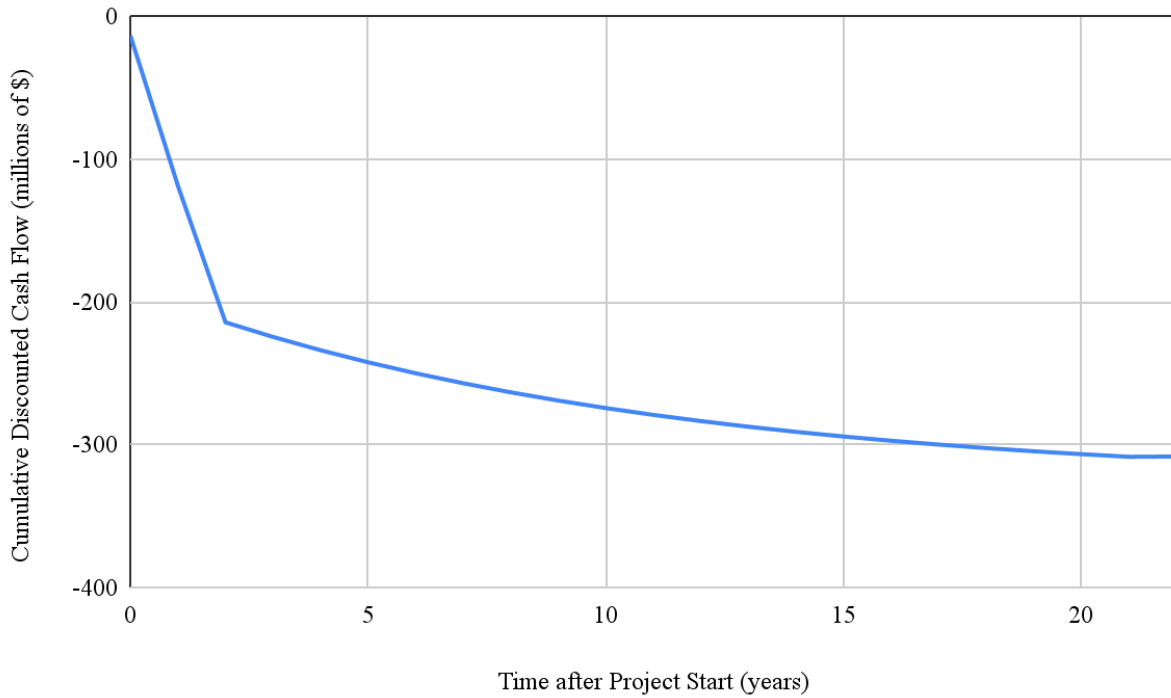


Figure 4-4-03: Cumulative Discounted Cash Flow Diagram (No Glycerol Refinement)

As shown by Table 4-4-06, the total number of operators and supervisors required does not change between the base scenario and this alternate scenario, since the total number of equipment removed is a fraction of what is required. The total capital and operating costs saved from eliminating the equipment involved in glycerol refinement is a fraction of the original capital and operating costs.

5. Safety and Environmental Concerns

5.1 Health and Safety Considerations

A major safety concern is the use of large quantities of methanol in the downstream process. Methanol vapors are both highly flammable and highly toxic to humans when inhaled, and can pose a serious threat in the event of a leak. Storage tanks containing methanol should be physically isolated from any sources of ignition or combustion, and there should be relief valves on any tanks that lead directly to a flare system.

As with any chemical process, this process has dangers associated with working in confined spaces. This may occur for numerous reasons, but a specific example is when process equipment needs to be maintained. When working in these confined conditions, asphyxiation is a major concern. In order to avoid this, solutions like continuous air monitoring, good ventilation, comprehensive training, and breathing air should be implemented. At the very least, anyone working on the plant should be trained to not break the plane of the vessel without knowing if it is safe or not.

Algae growth and cultivation does not have as many direct dangers as other areas of the process. However, there are some safety concerns specifically associated with the raceway ponds. One such concern is drowning. Even though the pond is not very deep at 0.4 m, a person could not be paying enough attention and easily fall into one of the raceway ponds, become unconscious, and drown.

There is enough sulfuric acid present in this process to consider it when assessing potentially dangerous situations that may occur. Sulfuric acid is an irritant, and it can also cause burns to the skin (PubChem, n.d.). As a result, caution should be used with any process that

involves it. The storage of the acid should be separated from other chemicals in order to prevent cross-contamination and violent reactions from occurring.

KOH is a hazardous material that is present in our process, so its associated hazards should be addressed. KOH is an irritant and is corrosive (PubChem, n.d.). This means that when someone comes into contact with KOH, whether by touch or inhalation, it could cause serious damage to them. KOH is not present in large quantities like some of the other hazardous materials in the process, but it still should be handled with care and used in a way that minimizes any contact that operators need to make with KOH. An inherently safer design minimizing the human interaction with KOH would help reduce the risk of an accident occurring.

This process involves a large amount of hexane, which presents its own array of safety concerns to deal with. Two major concerns associated with the use of hexane, especially in large quantities, are its flammability and the effects it has on people that are exposed to it (EPA, n.d.). Hexane can affect the central nervous system through short term exposure and cause polyneuropathy through long term exposure (EPA, n.d.). In order to minimize the risk of a significant event occurring, the amount of hexane that is stored on the premises should be kept to a minimum and there should be relief valves on any tanks that lead directly to a flare system. The relief valve feeding the flare should also help prevent human exposure to hexane by burning off any excess vapors.

There is the potential for fires to occur in this process, especially in the biodiesel purification portion. Due to the large amount of biodiesel being produced daily, a significant fire could occur. In order to help prevent a significant event from occurring, the amount of biodiesel that is stored on the premises should be kept to a minimum and there should be relief valves on any tanks that lead directly to a flare system.

5.2 Environmental Considerations

Around 196,700 tons of chicken litter and 148,800 tons of turkey litter can be recovered per year across four counties that lie in the Shenandoah Valley region. This plant plans to recover this amount of poultry litter, extract its nutrients and convert it into algae. This is beneficial to the environment due to preventing the poultry litter, which has a high nitrogen and phosphorous content, from washing into the waterway. If these nutrients were allowed to enter the waterway, it could cause major issues to occur, such as algae outbreaks, bacterial contamination, and other environmental and public health risks. (*Poultry Litter Problem*, 2020). Thus, it is better to use these nutrients for controlled algae growth. Further research is needed to see if there are any excess nutrients exiting the process and how to manage them if there are.

Greenhouse gasses will be removed from the atmosphere by the algae as it grows. The algae is being used to produce fuel that will be burned causing greenhouse gasses to be introduced into the atmosphere, but the carbon present in the algae was already in the atmosphere. This means that the fuel produced from the algae is different from burning fossil fuels that come from below ground and introduce new carbon into the atmosphere. Thus, the production of this fuel is overall positive in regards to the capture of carbon.

15.4 million acres, or 61% of the total land area, in Virginia is forests (Birch et al., 1998). As a result of this, it is likely that in most non-city and non-coastal areas there are forests or wooded areas dispersed throughout. 3,440 acres of land are needed for this plant, and most of that land is being used for the cultivation of algae in open raceway ponds. This is a significant amount of land, which means that it wouldn't naturally be in the necessary state for the construction of raceway ponds. Deforestation would likely have to occur in order to clear enough

land for this plant to be built. An attempt should be made to repurpose farmland for this plant in order to avoid this.

With the use of open raceway ponds, there is the possibility for the contamination from wild species to occur due to them being an open system. However, the open system also creates the possibility of local waterways being contaminated with the algae being used in the process. A leak in the system or flooding could allow for an excess amount of *Chlorella Vulgaris* to escape the plant and enter the local waterways. This could lead to *Chlorella Vulgaris* becoming more prominent in the natural waterways, killing off or overpowering the native species of algae. This could affect the ecosystem in adverse ways depending on how the native species fit into the various natural cycles in the area. The *Chlorella Vulgaris* could create the problem of an algae bloom occurring if the correct conditions were present.

If the sulfuric acid present in this process were to escape into the environment through a loss of containment, it could cause some fairly significant damages. Due to its corrosive nature, it would burn any plants, birds or land animals exposed to it (*Sulfuric Acid | National Pollutant Inventory*, n.d.). Sulfuric acid also has moderate chronic toxicity to aquatic life (*Sulfuric Acid | National Pollutant Inventory*, n.d.). The sulfuric acid will also enter the air and react with other chemicals that are present and will travel along air currents until wet acid deposition (acid rain, acid fog, etc) occurs, and it will also readily mix with water if allowed to enter the waterway (*Sulfuric Acid | National Pollutant Inventory*, n.d.). If the KOH present in this process were to escape into the environment through a loss of containment, it could also cause some environmental issues. Potassium hydroxide is moderately toxic to aquatic organisms, and it dissociates in water and can elevate the pH of systems that are not well buffered (OXY Occidental Chemical Corporation, n.d.).

This process has a total of 9 waste streams. The waste streams are 106, 307, 416, 508, 616, 705, 709, 805, and 809. It is important to handle these streams appropriately to minimize the risk of any adverse effects they have on the environment. Waste stream 106 is unique due to it being the solid portion of the poultry litter that did not dissolve in the water. Due to the nutrients being extracted from it, it may be safe to put this waste into a landfill, but until further research is done into the composition of this waste stream, burning it in a furnace may be a safer option for discarding it.

5.3 Societal Considerations

As mentioned in the prior section, the growth of algae requires an extensive amount of land. The land used for the growth of the algae could be put to many different uses, and it comes down to society placing importance on what they want to use the land for. The 3,440 acres of land needed for this project could also be used as farmland, land for residential construction, or land for commercial construction. This could lead to the surrounding community being upset with the construction of a biodiesel plant rather than these other options. However, the community may also view the construction of a biodiesel plant as being a more worthy use of the land than the other options, which could lead to the community supporting this plant and its operation.

The biodiesel production capacity in the United States was 2.24 billion gallons in 2021 (*U.S. Biodiesel Production Capacity 2021*, n.d.). The amount of biodiesel that was imported into the United States was 202,944,000 gallons in 2021 (*U.S. Biodiesel Imports*, n.d.). This plant has the capacity to produce 4,528,000 gallons per year. As a result, this plant does not have a significant contribution to the scale of production in the United States, but it will increase the fuel security of the United States by decreasing the amount of biodiesel that needs to be imported from other countries. The total amount of imported biodiesel needed would decrease by 2.23% if this plant were to begin production.

This plant as it is currently designed would create 107 jobs in Rockingham County, VA. 97 of these jobs will be as operators, with a salary of \$42,596. 10 of these jobs will be as supervisors, with a salary of \$60,000. With the median income of Rockingham County being \$30,700 (*Rockingham County - Place Explorer - Data Commons*, n.d.), it is clear that this plant

would create a significant number of jobs with reasonable salaries for the area. This would be beneficial to Rockingham County, for it would likely help slightly boost the economy in the area.

The algae produced in this process would have a strong musty, or rotting, odor associated with it if it were allowed to die, but this odor typically would not occur while the algae is living and has a more neutral or leafy scent (State Water Resources Control Board, n.d.). However, due to the algae cultivation being open to air, there is the possibility of contamination. If cyanobacteria were to get into the raceway pond system, then the smell would be much more unpleasant, and it would smell more like gas, septic, or fish (State Water Resources Control Board, n.d.). Due to this potential for a bad odor, people from the surrounding area may show opposition for the open raceway ponds near them.

6. Conclusions and Recommendations

After examination of the process conditions and economics of production, we cannot recommend that this project proceeds. While the initial reactions and attitudes towards algae biofuel technology may be positive, after factoring in the amount of land and water required for algae growth, as well as current diesel prices, it does not make economic sense to proceed with this project.

The largest obstacle in the project in its current state is the relative difficulty of efficiently producing massive quantities of the target algae strain. Open raceway ponds, while being more cost-effective overall, do not produce high biomass cultures. As a result, in order to grow the target quantity of algae, a disproportionately large amount of land and water are required for this process. This, combined with the fact that algae cultures must be dewatered before use in lipid extraction, results in an extremely inefficient, high energy process for producing a relatively low volume of biodiesel product. This is made evident when examining the economics of the plant, as upstream growth and processing comprises the vast majority of both the capital costs and daily operational costs of this project.

Overall, while this project may provide a societal benefit in the scope of carbon capture, providing an alternative to fossil fuels, creation of jobs, and poultry waste treatment, there are significant obstacles associated with this process, namely the massive scale of land use, net energy loss, and, most importantly, little to no return on investment. In order for this project to be lucrative, significant strides must be made in algae growth technology, as current methods use a very large number of resources to produce a low density algae culture.

7. Acknowledgements

We would like to acknowledge the help that Professor Anderson offered us throughout the year. His knowledge and insight never failed to guide us in the right direction while working on this project.

References

2.3: *LIQUID-LIQUID EXTRACTION*. (2019, February 10). Chemistry LibreTexts.

[https://chem.libretexts.org/Bookshelves/Organic_Chemistry/Book%3A_How_to_be_a_Successful_Organic_Chemist_\(Sandtorv\)/02%3A_COMMON_ORGANIC_CHEMISTRY_LABORATORY_TECHNIQUES/2.03%3A_LIQUID-LIQUID_EXTRACTION](https://chem.libretexts.org/Bookshelves/Organic_Chemistry/Book%3A_How_to_be_a_Successful_Organic_Chemist_(Sandtorv)/02%3A_COMMON_ORGANIC_CHEMISTRY_LABORATORY_TECHNIQUES/2.03%3A_LIQUID-LIQUID_EXTRACTION)

Adesanya, V. O., Cadena, E., Scott, S. A., & Smith, A. G. (2014). Life cycle assessment on microalgae biodiesel production using a hybrid cultivation system. *Bioresource Technology*, 163, 343-355. <http://dx.doi.org/10.1016/j.biortech.2014.04.051>

Ali, H., Cheema, T. A., & Park, C. W. (2018). Determination of the Structural Characteristics of Microalgal Cells Walls under the Influence of Turbulent Mixing Energy in Open Raceway Ponds. *Energies*, 11(2), 388. <https://doi.org/10.3390/en11020388>

Ariete Homogenizer 5400, powerful, reliable and versatile. (n.d.). GEA Engineering for a Better World. Retrieved March 4, 2022, from <https://www.gea.com/en/products/homogenizers/industrial-homogenizers/homogenizer-Ariete-5400.jsp>

Arrora, A., Baroi, C., & Dalai, A. K. (2015). Feasibility of Crude Glycerol Purification Process. *Journal of Basic and Applied Engineering Research*, 2(1), 60-63.

Available In Multiple 2021 Hot Selling Strong Flexibility Super Clear Transparent Soft Pvc Sheet Custom Size Pvc Flexible Film—Buy Reliable Chinese Plastic Manufacturers Colorful 2mm Transparent Soft Pvc Sheet Custom Size Pvc Flexible Film Roll For Windows,China Factory Export Colourful Transparent Soft Pvc Sheet Custom Size Pvc Shrink Flexible Films Roll For Table Cloth,Different Thicknesses Coloured High Transparency Soft Pvc Sheet Custom Size Printed Flexible Films Roll For Packing Soft Bags Product on Alibaba.com. (n.d.). Retrieved April 14, 2022, from https://www.alibaba.com/product-detail/Available-In-Multiple-2021-Hot-Selling_60768175655.html?spm=a2700.7724857.normal_offer.d_title.3281391fVnlMif

Berry, J. (2020, December 15). *How much does it cost to fill a swimming pool with water? (with calculator)*. Easy Clear Pool. Retrieved April 15, 2022, from <https://easyclearpool.com/how-much-does-it-cost-to-fill-a-swimming-pool/>

Birch, T. W., Hodge, S. S., & Thompson, M. T. (1998). Characterizing Virginia's private forest owners and their forest lands. (NE-RP-707; p. NE-RP-707). U.S. Department of Agriculture, Forest Service, North Central Research Station. <https://doi.org/10.2737/NE-RP-707>

Carreira, R. I., Goodwin, H. L., & Hamm, S. J. (n.d.). How Much Is Poultry Litter Worth? 20. Cepci Index 1950—2015. (n.d.). Pdfcoffee.Com. Retrieved April 14, 2022, from <https://pdfcoffee.com/cepci-index-1950-2015-pdf-free.html>

Chastain, J. P., Camberato, J. J., & Skewes, P. (2003). Poultry Manure Production and Nutrient Content. In CAMM Poultry Training Manual. Clemson University.

Chemical Plant Operator I Salary in Virginia | Salary.com. (n.d.). Retrieved April 14, 2022, from <https://www.salary.com/research/salary/benchmark/chemical-plant-operator-i-salary/va>

Chisti, Y. (2013). Raceways-based Production of Algal Crude Oil. *Green*, 3(3–4), 195–216. <https://doi.org/10.1515/green-2013-0018>

Climate in Rockingham County, Virginia. (n.d.). <https://www.bestplaces.net>. Retrieved February 18, 2022, from <https://www.bestplaces.net/climate/county/virginia/rockingham>

Daf Dissolved Air Flotation System Water Treatment Equipment For Environmental Protection Equipment Flotation De Gas Disuelto—Buy Flotation De Gas Disuelto,Dissolved Air Flotation Clarifier,Dissolved Air Flotation System Water Treatment Equipment For Environmental Protection Equipment Product on Alibaba.com. (n.d.). Retrieved April 14, 2022, from https://www.alibaba.com/product-detail/Dissolved-Air-Flotation-DAF-Dissolved-Air_1600286858286.html?spm=a2700.galleryofferlist.normal_offer.d_title.3eb7395c19C4r4&s=p

de Vree, J. H., Bosma, R., Janssen, M., Barbosa, M. J., & Wijffels, R. H. (2015, December 18). *Comparison of four outdoor pilot-scale photobioreactors - biotechnology for biofuels and Bioproducts*. BioMed Central. Retrieved May 6, 2022, from <https://biotechnologyforbiofuels.biomedcentral.com/articles/10.1186/s13068-015-0400-2#:~:text=of%20direct%20light.-,Flat%20panel%20photobioreactor,m%20distance%20betwe en%20the%20panels>.

Diesel prices around the world, 11-Apr-2022. (n.d.). GlobalPetrolPrices.Com. Retrieved April 14, 2022, from https://www.globalpetrolprices.com/diesel_prices/

Ellison, H. (2021). Virginia 2021 Farm Real Estate Value and Cash Rent. Lancaster Farming. Retrieved April 14, 2022, from https://www.lancasterfarming.com/news/main_edition/virginia-2021-farm-real-estate-value-and-cash-rent/article_07ef927d-b699-5e91-bd91-2ad2c7cf1390.html

EPA. (n.d.). *Hexane*. <https://www.epa.gov/sites/default/files/2016-09/documents/hexane.pdf>

European Biofuels Technology Platform. (2011). Fatty Acid Methyl Esters. <https://www.etipbioenergy.eu/images/fame-fact-sheet.pdf>

Farm-Energy. (2019, April 12). *New uses for crude glycerin from biodiesel production*. Farm Energy. Retrieved April 14, 2022, from <https://farm-energy.extension.org/new-uses-for-crude-glycerin-from-biodiesel-production/>

Farobie, O. (2016, January 19). *Application of spiral reactor for biodiesel production in supercritical methanol and ethanol: Process evaluation*.

Fears, D. (2017). Nearly 200 million chickens, turkeys and cows are making a mess of the Shenandoah River. *Washington Post*. Retrieved October 7, 2021, from <https://www.washingtonpost.com/news/energy-environment/wp/2017/04/26/nearly-200-million-chickens-turkeys-and-cows-are-making-a-mess-of-the-shenandoah-river/>

Find quality Manufacturers, Suppliers, Exporters, Importers, Buyers, Wholesalers, Products and Trade Leads from our award-winning International Trade Site. Import & Export on alibaba.com. (n.d.). Alibaba. Retrieved April 14, 2022, from <https://www.alibaba.com>

Gea Homogenizer. (n.d.). Indiamart.Com. Retrieved April 14, 2022, from <https://www.indiamart.com/proddetail/gea-homogenizer-22809298573.html>

- Glisic, S., & Skala, D. (2009). Design and optimization of purification procedure for biodiesel washing. *Chemical Industry and Chemical Engineering Quarterly*, *15*(3), 159-168.
<https://doi.org/10.2298/ciceq0903159g>
- Günerken, E., D'Hondt, E., Eppink, M. H. M., Garcia-Gonzalez, L., Elst, K., & Wijffels, R. H. (2015). Cell disruption for microalgae biorefineries. *Biotechnology Advances*, *33*(2), 243–260. <https://doi.org/10.1016/j.biotechadv.2015.01.008>
- Halim, R., Harun, R., Danquah, M. K., & Webley, P. A. (2012). Microalgal cell disruption for biofuel development. *Applied Energy*, *91*(1), 116–121.
<https://doi.org/10.1016/j.apenergy.2011.08.048>
- Harrisonburg December Weather, Average Temperature (Virginia, United States)—Weather Spark. (n.d.). Retrieved February 18, 2022, from <https://weatherspark.com/m/20236/12/Average-Weather-in-December-in-Harrisonburg-Virginia-United-States#Figures-SolarEnergy>
- He, Q., Yang, H., & Hu, C. (2016). Culture modes and financial evaluation of two oleaginous microalgae for biodiesel production in desert area with open raceway pond. *Bioresource Technology*, *218*, 571–579. <https://doi.org/10.1016/j.biortech.2016.06.137>
- Hosseinizand, H., Sokhansanj, S., & Lim, C. J. (2018). Studying the drying mechanism of microalgae *Chlorella vulgaris* and the optimum drying temperature to preserve quality characteristics. *Drying Technology*, *36*(9), 1049–1060. <https://doi.org/10.1080/07373937.2017.1369986>
- [Hot Item] 8PCS Impellers 2 HP Paddle Wheel Aerator. (n.d.). Made-in-China.Com. Retrieved April 14, 2022, from <https://geyinco.en.made-in-china.com/product/EvWmwQVGIDUA/China-8PCS-Impellers-2-HP-Paddle-Wheel-Aerator.html>

How does the corporate income tax work? (n.d.). Tax Policy Center. Retrieved April 14, 2022, from <https://www.taxpolicycenter.org/briefing-book/how-does-corporate-income-tax-work>

Learn how much it costs to Install a Pond. (n.d.). Retrieved April 14, 2022, from <https://www.homeadvisor.com/cost/landscape/install-a-pond/>

Menges, K. S. (2003). *Design and modeling of a vacuum drying system for a biodiesel pilot plant* [Master's thesis]. <https://dr.lib.iastate.edu/server/api/core/bitstreams/0bf14d98-42c2-45b5-9774-246feeb769ad/content>

Mujitaba, G., Choi, W., Lee, C., & Lee, K. (2012). *Lipid production by *Chlorella vulgaris* after a shift from nutrient-rich to nitrogen starvation conditions*. <https://doi.org/10.1016/j.biortech.2012.07.057>

Musa, I. A. (2016). The effects of alcohol to oil molar ratios and the type of alcohol on biodiesel production using transesterification process. *Egyptian Journal of Petroleum*, 25(1), 21-31. <https://doi.org/10.1016/j.ejpe.2015.06.007>

National Center for Biotechnology Information. (2021). PubChem Compound Summary for CID 753, Glycerol. <https://pubchem.ncbi.nlm.nih.gov/compound/Glycerol>

Narala, R. R., Garg, S., Sharma, K. K., Thomas-Hall, S. R., Deme, M., Li, Y., & Schenk, P. M. (2016, August 2). *Comparison of Microalgae cultivation in Photobioreactor, open raceway pond, and a two-stage hybrid system*. *Frontiers*. <https://doi.org/10.3389/fenrg.2016.00029>

- Niaghi, M., Mahdavi, M. A., & Gheshlaghi, R. (2015). Optimization of dissolved air flotation technique in harvesting microalgae from treated wastewater without flocculants addition. *Journal of Renewable and Sustainable Energy*, 7(1), 013130.
<https://doi.org/10.1063/1.4909541>
- Nwanya, K. O., Okoye, P., & Ajiwe, V. (2021). Biodiesel Potentials of *Chlorella vulgaris* Oil. *Nigerian Research Journal of Chemical Sciences*, 9(2), 36-46.
<https://www.unn.edu.ng/wp-content/uploads/2021/07/Biodiesel-Potentials-of-Chlorella-vulgaris-Oil.pdf>
- OXY Occidental Chemical Corporation. (n.d.). *Potassium Hydroxide*. <https://www.oxy.com/globalassets/documents/chemicals/stewardship/potassium-hydroxide.pdf>
- Oliveira, M., Ramos, A., Monteiro, E., & Rouboa, A. (2022). Improvement of the crude glycerol purification process derived from biodiesel production waste sources through computational modeling. *Sustainability*, 14(3), 1747. <https://doi.org/10.3390/su14031747>
- Ozer, Richard W. (2014). *Green Vegetable Oil Processing || Algae Drying and Extraction*. , 81–105. doi:10.1016/b978-0-9888565-3-0.50008-x.
- Patel, S., & Kannan, D. C. (2021). A method of wet algal lipid recovery for biofuel production. *Algal Research*, 55, 102237. <https://doi.org/10.1016/j.algal.2021.102237>
- Poultry Litter Problem. (2020, June 24). Potomac Riverkeeper Network. <https://www.potomacriverkeepernetwork.org/poultry-litter-problem/>
- PubChem. (n.d.). Potassium hydroxide. Retrieved April 14, 2022, from <https://pubchem.ncbi.nlm.nih.gov/compound/14797>
- PubChem. (n.d.). Sulfuric acid. Retrieved April 14, 2022, from <https://pubchem.ncbi.nlm.nih.gov/compound/1118>

- Rahman, M. A., Aziz, M. A., Al-khulaidi, R. A., Sakib, N., & Islam, M. (2017). Biodiesel production from microalgae *Spirulina maxima* by two step process: Optimization of process variable. *Journal of Radiation Research and Applied Sciences*, *10*(2), 140–147. <https://doi.org/10.1016/j.jrras.2017.02.004>
- Rockingham County—Place Explorer—Data Commons. (n.d.). Retrieved April 14, 2022, from https://datacommons.org/place/geoId/51165?utm_medium=explore&mprop=income&pop=Person&cpv=age%2CYears15Onwards&hl=en
- Rodolfi, L., Zittelli, G. C., & Bassi, N. (2008). Microalgae for Oil: Strain Selection, Induction of Lipid Synthesis and Outdoor Mass Cultivation in a Low-Cost Photobioreactor. *Biotechnology and Bioengineering*, *102*(1), 100-112. <https://doi.org/10.1002/bit.22033>
- Rogers, D. W., Hoyte, O. P. A., & Ho, R. K. C. (1978). *Heats of hydrogenation of large molecules. Part 2. Six unsaturated and polyunsaturated fatty acids*. *74*, 46–52.
- Rogers, D. W., & Choudhury, D. N. (1978). Heats of hydrogenation of large molecules. Part 3—Five simple unsaturated triglycerides (triacylglycerols). *74*, 2868–2872.
- Rosenberg, J. N., Mathias, A., Korth, K., Betenbaugh, M. J., & Oyler, G. A. (2011). Microalgal biomass production and carbon dioxide sequestration from an integrated ethanol biorefinery in Iowa: A technical appraisal and economic feasibility evaluation. *Biomass and Bioenergy*, *35*(9), 3865–3876. <https://doi.org/10.1016/j.biombioe.2011.05.014>
- Roque, T. V., Correia, M. J. N., & Carvalho, R. (n.d.). *Analysis of the Hexane Loss in a Vegetable Oil Extraction Unit*. *10*.
- Ru, I. T. K., Sung, Y. Y., Jusoh, M., Wahid, M. E. A., & Nagappan, T. (2020). *Chlorella vulgaris*: A perspective on its potential for combining high biomass with high value bioproducts. *Applied Phycology*, *1*(1), 2–11. <https://doi.org/10.1080/26388081.2020.1715256>

Sedimentation Tank Design Parameters. (2018, March 13). The Constructor.

<https://theconstructor.org/environmental-engg/sedimentation-tank-design-parameters/21277/>

Sim, T.-S., Goh, A., & Becker, E. W. (1988). Comparison of centrifugation, dissolved air flotation and drum filtration techniques for harvesting sewage-grown algae. *Biomass*, 16(1), 51–62. [https://doi.org/10.1016/0144-4565\(88\)90015-7](https://doi.org/10.1016/0144-4565(88)90015-7)

State Water Resources Control Board, (n.d.). *Identifying a Harmful Algal Bloom* [PowerPoint slides]. California Water Boards, https://mywaterquality.ca.gov/habs/what/visualguide_fs.pdf

Sulfuric acid | National Pollutant Inventory. (n.d.). Retrieved April 14, 2022, from <http://www.npi.gov.au/resource/sulfuric-acid>

Suwannakarn, K., Lotero, E., Ngaosuwan, K., & Goodwin, J. G. (2009). Simultaneous free fatty acid esterification and triglyceride Transesterification using a solid acid catalyst with in situ removal of water and Unreacted methanol. *Industrial & Engineering Chemistry Research*, 48(6), 2810-2818. <https://doi.org/10.1021/ie800889w>

Tax Rates | Rockingham County, VA - Official Website. (n.d.). Retrieved April 14, 2022, from <https://www.rockinghamcountyva.gov/202/Tax-Rates>

Trambouze, P., van Landeghem, H., & Wauquier, J. P. (1988). *Chemical Reactors: Design, Engineering, Operation*. Gulf Publishing Company. <https://books.google.com/books?id=e7rpAAAAMAAJ>

Turton, R., Shaeiwitz, J. A., Bhattacharyya, D., & Whiting, W. B. (2018). *Analysis, Synthesis, and Design of Chemical Processes* (5th ed.). O'Reilly.

U.S. Biodiesel Imports. (n.d.). Retrieved April 14, 2022, from https://www.eia.gov/dnav/pet/pet_move_impcus_a2_nus_EPOORDB_im0_mdbl_a.htm

- U.S. biodiesel production capacity 2021. (n.d.). Statista. Retrieved April 14, 2022, from <https://www.statista.com/statistics/520072/us-annual-production-capacity-biodiesel-per-month/>
- U.S. Department of Energy. (n.d.). Alternative fuels data center: ASTM biodiesel specifications. https://afdc.energy.gov/fuels/biodiesel_specifications.html
- “U.S. Energy Information Administration - EIA - Independent Statistics and Analysis.” *Today in Energy - Daily Prices - Prices - U.S. Energy Information Administration (EIA)*, <https://www.eia.gov/todayinenergy/prices.php>.
- U.S. International Trade Commission. (2017). Biodiesel From Argentina And Indonesia: Investigation Nos. 701-TA-571-572 (Final) (4748). https://www.usitc.gov/publications/701_731/pub4748.pdf
- Vassilev, S. V., & Vassileva, V. G. (2016). Composition, properties and challenges of algae biomass for biofuel application: An overview. *Fuel*, 181, 1-33. <https://doi.org/10.1016/j.fuel.2016.04.106>
- Virginia State Income Tax. (n.d.). [Www.Nolo.Com](https://www.nolo.com/legal-encyclopedia/virginia-state-income-tax.html). Retrieved April 14, 2022, from <https://www.nolo.com/legal-encyclopedia/virginia-state-income-tax.html>
- Yap, B. H. J., Crawford, S. A., Dumsday, G. J., Scales, P. J., & Martin, G. J. O. (2014). A mechanistic study of algal cell disruption and its effect on lipid recovery by solvent extraction. *Algal Research*, 5, 112–120. <https://doi.org/10.1016/j.algal.2014.07.001>